Radar Scatterometry---
An Active Remote Sensing Tool

by

R. K. MOORE

CRES Report No. 61-11

A paper presented to the Fourth Symposium on Remote Sensing of the Environment, University of Michigan, Ann Arbor, Michigan, April 11-14, 1966.

Supported by

NASA Contract NSR 17-004-003

CRES

THE UNIVERSITY OF KANSAS • CENTER FOR RESEARCH INC
ENGINEERING SCIENCE DIVISION • LAWRENCE, KANSAS

RADAR SCATTEROMETRY -- AN ACTIVE REMOTE SENSING TOOL

by

R. K. Moore

CRES Report No. 61-11

A paper presented to the Fourth Symposium on Remote Sensing of the Environment, University of Michigan, Ann Arbor, Michigan, April 11-14, 1966.

Supported by

NASA Contract NSR 17-004-003

RADAR SCATTEROMETRY --

AN ACTIVE REMOTE SENSING TOOL

R. K. Moore

Center for Research in Engineering Science
University of Kansas
Lawrence, Kansas

36083

ABSTRACT

The radar scatterometer measures variation of the radar scattering coefficient with angle, wavelength, and polarization. These variations may be used by geoscientists to discriminate between surfaces with different roughness and materials. For example, such a system has been proposed to determine from a satellite the height of ocean waves, and from this to infer the wind field over the world's oceans.

Radar scatterometers may be built using different combinations of angle, range, and speed measurement to discriminate among surface elements. Various systems are described, but only the range-angle system is studied in detail. The sizes of the areas sampled and the size of sample required for adequate statistics are described. Various data presentation methods are suggested.

1. INTRODUCTION

Radar scatterometers permit more detailed observation of radar scattering behavior than radar imagers in the same way that infra-red spectrometers permit more detailed observation than infra-red imagers. The penalty paid for this information gain is degraded resolution and reduced areal coverage. Radar scatterometers measure variation of scattering coefficient with angle for radar signals. Some scatterometers, like some other radar systems, permit studying the effect of polarization and wavelength variations.

Applications of radar scatterometry to measuring sea-state and ice roughness have been established. Applications over land are speculative because suitable measurements have not been made. However, indications are that terrain texture and moisture content, not only at the surface but somewhat beneath it, may be observed by radar scatterometers with different scales than by other instruments.

Previous radar scatterometry measurements have almost all been motivated by the need for the radar design information. Most measurements have been in relatively short programs planned to obtain specific information for a design. Some have been conducted over longer periods and more carefully than the short programs, but the lack of geoscience motivation has limited the amount of ground truth information obtained, except in the detailed measurements made by Ohio State University. Accordingly, techniques for making the measurements have been developed much further than data interpretation.

Radar scatterometers, like other radar systems, can take advantage of both range and velocity measurements to discriminate areas on the ground by combinations of antenna pattern and range, antenna pattern and velocity, or range and velocity measurement. Furthermore, the methods for measuring range and velocity are varied. This paper discusses some of the general concepts for such systems.

A range-angle "fan beam" scatterometer system is discussed in detail, using somewhat idealized assumptions. Resolution along the flight track varies from quite a large resolution distance at the vertical to quite a small one at angles approaching the grazing. Conversely, the resolution distance across the track varies from a minimum at the vertical relatively slowly out to about 60° and quite rapidly thereafter. Even though along-track resolution distance for angles near grazing is

extremely small compared with the distance near the vertical, averaging required to obtain an accurate measurement requires a larger effective resolution distance that approaches that near the vertical.

Velocity-angle systems have a different set of problems as variation of resolution distances along the flight track is opposite to that with the range-angle systems. The velocity measuring systems are not treated in detail here.

Use of the fan beam system requires processing of the data after flight because observations are made simultaneously from different terrain elements at different incident angles, and the observations for a particular terrain element must be collated later. After this has been done, a curve of scattering coefficient vs. angle may be plotted for each terrain element. However, such curves are difficult to analyze and other means are proposed for presenting the results on overlays to be used with maps and photographs.

2. SCATTEROMETER SYSTEM DESCRIPTIONS

Scatterometers may take numerous forms because of the many types of measurements possible with radar. Here we describe the function of a scatterometer, and the principles of the basic system types. Details are reserved for later sections.

2.1. WHAT A SCATTEROMETER MEASURES

A scatterometer measures the scattering or reflective properties of surfaces (and sometimes of volumes). A radar scatterometer measures reflection and scattering of waves generated by the radar itself. Since for most radar sets the transmitter and receiver are in the same place, most scatterometers measure signals returned to the source. Most signals are returned to the receiver by a scattering process. Only occasionally does specular reflection contribute significantly to the radar return. Hence, the term "scatterometer" is more appropriate than the term "reflectometer."

Most scatterometers measure the variation of differential scattering cross section of a surface with angle of incidence. The angle of incidence may vary from zero (normal incidence) to 90° (grazing incidence). Few scatterometer systems operate over the entire angular range. Airborne scatterometers of the type discussed here may operate near normal incidence, but they have difficulty at grazing incidence because at these angles the range is so great that the signals received are too small.

Some scatterometers transmit and/or receive with different polarizations. For example, a scatterometer may transmit horizontal and receive both vertical and horizontal polarization, or it may transmit first one and then the other polarization, receiving both with each transmission. Circular polarization may also be used.

Most scatterometers use only a single carrier frequency. However, measurement of scattering properties over a wide range of frequencies provides additional information, and certainly scatterometers of the future will do this.

An ordinary imaging radar measures scattering coefficient if it is calibrated properly, but it can do so for any point in the image at only the particular angle of incidence with which that point is illuminated. Most scatterometers obtain more information than this by measuring the scattering properties at various angles.

The scatterometer, like other radar sets, contains the basic elements shown in Figure 1. A transmitter sends a signal to the surface being studied. The signal is scattered to the receiver. Some sort of synchronization is maintained between transmitter and receiver; in fact, a copy of the transmitted signal may be delayed and compared in the receiver with the received signal. The receiver output is processed to determine the scattering coefficient at a particular point and the result is displayed. Radar systems for other purposes have the same elements.

2.2. CONTROL OF AREA SENSED

Radar scatterometers, since they provide their own illumination, can take advantage of knowledge about the illumination to discriminate among the returning signals. Systems dependent upon self-emission from the surface or upon scattering of incident radiation from other sources do not have this advantage. Figure 2 illustrates the ways radars determine the area sensed.

Figure 2a shows control of the illumination and discrimination of the returns by angular measurements only. That is, the antenna pattern is used to determine the surface element observed. Non-radar measurements of reflectivity, scattering, or emission are restricted to use of this method only. The size of the illuminated area is determined by the size (in wavelengths) of the aperture. Thus, for the longer wavelengths, it is difficult to get an aperture enough wavelengths across to confine the sensed area to a small size.

Figure 2b illustrates the first unique property of the radar -- its ability to measure range. By comparing a signal received with a delayed copy of the transmitted signal, one can select that part of the received signal that was delayed the same amount. Because the electromagnetic wave travels at a known velocity, each delay time is associated with a given range, or distance from radar to target to radar. Such range measurements are limited by the ability to determine the difference between signals experiencing different delays. A radar in an aircraft is pictured and it is assumed that the antenna pattern is isotropic. Hence, the only discrimination possible is the range discrimination. The locus of points on a plane surface at constant range from the radar is a circle. Hence, a pair of concentric circles limits the region contributing to the signal received at a particular time. If the range discriminating ability of the radar is improved, the circles are closer together.

Combination of the angular discrimination of Figure 2a with the range discrimination of Figure 2b permits further restriction of the area, as indicated in Figure 2c. Most radar systems in use employ this technique. Range discrimination is usually limited by the finite (non-zero) length of a transmitted pulse. Angular discrimination is determined by the size of the antenna.

If the radar is in motion over the plane the received frequency differs from the transmitted frequency by the amount of the Doppler shift. This is given by

$$f_d = \frac{2\underline{v} \cdot \underline{1}_R}{\lambda} \tag{1}$$

where $\underline{v}$ is the radar velocity;

$\underline{1}_R$ is the unit vector from radar to target element;

and λ is the wavelength.

The relative speed is determined by variations in the angle between $\underline{v}$ and $\underline{1}_R$. For horizontal travel, loci of constant relative speed and hence constant Doppler frequency are hyperbolas, as shown in Figure 2d.

A Doppler measurement system with no angle and range discrimination distinguishes the area that is contained between the lines of constant Doppler frequency representing the limits of a filter pass band. Hence, it is a strip between two hyperbolas. Either angular discrimination by antenna pattern or range discrimination may be used with the Doppler frequency discrimination to confine the observed area to a small region. The region determined by a narrow antenna beam pointed in the direction of radar travel and two lines of constant Doppler frequency is designated A. If the antenna beam were narrow and pointed normal to the direction of travel, the constant antenna gain lines and constant Doppler lines would be parallel and little discrimination would occur.

Along the flight path, however, lines of constant range and constant Doppler frequency are almost parallel. Hence, a system using range discrimination and Doppler frequency discrimination works best for an area such as B.

Any combination of the area discrimination systems shown in Figure 2 can be used to develop a scatterometer. The next three sections describe systems using different pairs of these measurements.

2.3. RANGE-ANGLE SYSTEMS

Figure 2c illustrates the combination of range and angle discrimination. A radar system may achieve range discrimination by any scheme permitting comparison of a received signal with a delayed version of a modulation signal -- with the amount of delay determining the range from which the received signal will be selected. Transmitting a pulse of short duration is the most common method. If the pulse is delayed and used to turn on the receiver at a later time, the output of the receiver is the signal scattered from the distance for which the round trip signal travel time in space is equal to the delay.

A typical range-angle system uses an antenna with a fan-shaped beam that is narrow in the direction transverse to the flight path and wide along the flight path. Figure 3 shows a contour on the ground of points seen with the same gain by the antenna. It may be treated as the limit of the illuminated ground area. Shown within this contour are sections of the circles of constant range; thus area A is selected if the distance between the two iso-range contours is the length of a transmitted pulse and the internal pulse delay is the same as that for a signal returned from the outer contour. Use of a different delay would select an area between another pair of iso-range contours.

The iso-range contours can also be set by frequency modulating the radar or by using other types of modulation such as quasi-random binary phase modulation.

With any range measurement systems, the block diagram in Figure 4 is applicable. Modulation in amplitude, frequency, or phase is applied to a transmitter. The output of the transmitter is fed to an antenna which radiates toward the ground. At the same time a sample of the modulator output is sent to a delay unit. The signal coming from the transmitter antenna goes to the ground and is returned to the receiver antenna. The output of the receiver and the output of the modulation delay unit go to a modulation comparator. The comparator output is due to signals scattered from the range for which the delay unit is set and receiver outputs from other ranges are not transmitted. Thus, if only a single delay is used, the output of the modulation comparator is an amplitude corresponding to a certain range. Normally the modulation delay unit has numerous delays possible, so the output of the modulation comparator is a set of information on amplitude vs. range, with the number of range points being determined by the number of separate delays.

With a pulse or binary phase coded system, range and time are ordinarily directly related so the output also is in the form of amplitude vs. time. With an FM system, range and frequency are related so the output is in the form of an amplitude vs. frequency.

Although separate antennas are shown, many systems use the same antenna for transmitting and receiving.

2.4. VELOCITY-ANGLE SYSTEMS

The principle illustrated by element A in Figure 2d permits separation of ground elements within the angular confines of a beam by measurement of velocity. Figure 5 shows the ground map of this process. Here, again, a fan-beam antenna has been assumed. The area within the iso-gain contour shown is considered illuminated and that outside the iso-gain contour is considered dark. Area A is further restricted by a filter separating out a particular range of Doppler frequencies.

Figure 6 shows a block diagram of such a system. The fundamental velocity-angle system does not use modulation; hence, the modulation block that was present in Figure 4 does not appear in Figure 6. The carrier frequency may be delayed or the carrier frequency being transmitted at the time the signal is received may be used in the phase comparator. The output of the phase comparator is a spectrum of Doppler frequencies. Since each frequency is associated with a given relative speed, this output is a measure of amplitude vs. relative speed. Separating the various frequencies with filters permits separation of the areas on the ground.

2.5. RANGE-VELOCITY SYSTEMS

Explanation of simultaneous range and velocity measurements requires illustration of both iso-velocity contours and iso-range contours as indicated in Figure 7. Of course, some sort of antenna is also present so an iso-gain contour is shown to limit the other contours. The area A, however, is not determined by the iso-gain contour. It is bounded by two iso-velocity contours and two iso-range contours. It may be set by any of the range measurement schemes combined with Doppler frequency measurements.

Figure 8 illustrates a simplified block diagram of a range-velocity system. Here the modulation is shown feeding the transmitter and a sample of the modulated transmitter output is fed to the delay unit. This modulated output contains both the phase information necessary for Doppler measurement and the modulation information necessary for range measurement. The transmitter output goes to the antenna, is radiated to the ground, and re-radiated to the receiving antenna. At the output of the receiver a phase and modulation comparator appears. Its output gives the amplitude of the return as a function of range (usually expressed as time), and as a function of relative speed (usually expressed as Doppler frequency). By a combination of time and frequency filtering, therefore, the area A of Figure 7 can be separated from the composite return that contains many of such areas.

A real system of this kind may have several internal paths between transmitter and receiver. The modulation and phase reference may be separate from both transmitter and receiver but connected to both. Nevertheless, the principle illustrated in Figure 8 still applies.

Systems like this are commonly used as synthetic aperture side-looking airborne radars. Most scatterometers use forward looking systems, but a side-looking scatterometer based on this principle has been proposed for use in a meteorological spacecraft for sea-state observation.

2.6. SYSTEM CHOICE

For most uses, a scatterometer should obtain as much of the curve of scattering coefficient vs. angle of incidence as possible. If this curve is to be measured for a particular segment of ground, it is necessary that this segment be illuminated successively from different angles as the scatterometer moves. If the range of angles is to include the vertical, the scatterometer must fly directly over the illuminated segment. If the scatterometer is flying in a straight line, this requires that the illuminated area be centered along the flight track. Figure 9 illustrates this point. Here a pulsed (or other range-measuring) scatterometer is traveling over a plane surface. At angle θ_4 a first

observation is made of a particular segment of ground. Later, as the satellite advances, the same segment will be seen at an angle θ_3. Still later it will be seen at angle θ_2, later yet at angle θ_1, and finally the satellite will go directly over it. If the antenna pattern extends out the back, the sequence is then repeated in reverse order. If the antenna beam had been pointed in any other direction, it would not have been possible to obtain the vertical incidence record.

Since antenna pattern is the only good way to limit an area to small distances either side of the flight track, a fan-beam antenna illuminating a strip on the ground as shown in Figure 9 is the most useful for scatterometry. A single narrow beam could be used; it could be pointed ahead at a particular segment of ground and kept pointed at that segment as the radar travels toward and over the segment. Such a system only permits observation of selected points rather than a continuous track. Furthermore, it calls for accurate tracking of the same point on the ground by an antenna beam. Hence, for most purpose, it is inferior to the fan beam.

When a fan-beam system has been selected, the choice must be made between range and velocity measurement. As indicated in later sections, each has its advantages. The range measurement makes difficult discrimination between small angles near the vertical. The Doppler measurement, on the other hand, complicates matters away from the vertical. Detailed studies of system choices give answers that depend on particular problems being attacked, and are beyond the scope of this paper.

If a ranging system is chosen, a choice must be made between a pulse system and a frequency-modulated system or other CW or nearly-CW system.

For many purposes, the high peak powers of the pulse system cause problems. Furthermore, fast pulse circuits necessary to separate ranges with a pulse system can become rather complicated. On the other hand, the FM system depends on isolation between transmitter and receiver antennas if long range operation is contemplated. Such isolation is easy to achieve at relatively short wavelengths on large vehicles, but difficult on longer wavelengths and smaller vehicles.

If a velocity measurement system is to be used, a continuous-wave system is possible provided antenna isolation can be achieved. If this is not possible, some sort of an interrupted-CW system must be used so that the transmitter is turned off during the time the signal is being received. The CW-Doppler system is certainly the easiest system to build.

It is often desirable to measure range for other purposes. For example one may wish to use the same system for an altimeter and a scatterometer. Here, the CW or ICW system will not work. However, velocity measurement can be made in a suitably designed ranging system, for the Doppler shift exists regardless of the type of modulation used. Such Doppler measurements may or may not be worth the trouble, even where other conditions permit them.

At the longer wavelengths, a side-looking system using range and velocity measurement can get by with a considerably smaller antenna than any other system. For this reason, it is desirable any time only one angle of incidence is required. Although this may be the case of sea-state measurement, it probably will never be the case over land, where more parameters determine the return, so the additional information associated with different angles is necessary.

3. BASIS FOR SCATTEROMETER PERFORMANCE

Radar scattering coefficients vary differently with angle for different materials observed at different wavelengths and with different polarizations. These relations form the basis for scatterometry as a tool for the earth sciences.

Only a brief summary of the nature of experimental observations and theoretical predictions is given here. Details may be found in the references.

3.1. RADAR SCATTERING

Signals radiated by the transmitter of a radar are re-radiated by the ground and received back at the radar. If the ground surface is a perfectly smooth plane or sphere, a specular reflection results. For a specularly reflected signal to return to the radar, the surface (or a plane tangent to it) must be normal to the incident ray. Surfaces that are smooth enough to give specular reflection at wavelengths of a meter or less almost never occur in nature, and man-made surfaces this smooth are rare. Thus, radar return is almost always a scattering process.

The radar signal is made up of component signals re-radiated from numerous small scatterers and simultaneously observed by the radar. The average power received is the sum of the powers received from the individual scatterers. If specular reflection is involved, relative phase must also be taken into account; but for most targets of interest to earth science, the scattering process permits

summing the powers of contributions from different elements (without regard to phase). The radar equation describing this process is

$$\overline{P}_r = \sum_i \frac{P_t G^2 \lambda^2 \sigma_i}{(4\pi)^3 R_i^4} = \frac{P_t G^2 \lambda^2 \sigma^\circ \Delta A}{(4\pi)^3 R^4} \qquad (2)$$

where $\overline{P}_r$ is the average received power (watts)

P_t is the transmitted power (watts)

G is the antenna gain (same antenna assumed for transmitter and receiver)

λ is the wavelength (meters)

R_i is the range from radar to target element i (meters)

σ_i is the effective cross section of target element i (square meters).

The effective cross section, σ_i, is a number that describes the ability of the individual target element to re-radiate toward the radar. It includes the effects of absorption and of the angular distribution of re-radiation. This quantity can be calculated for simple target elements such as dielectric spheres, but is difficult to calculate for more complex target elements.

Most radar targets of earth-science interest are parts of a surface. Normally, the radar cannot discriminate individual elements on the surface having cross section σ_i, but must look at a sum of returns from many such elements. Rather than attempt to describe the individual scattering cross sections of the portions of the target, a scattering cross section per unit area of the surface (differential scattering cross section) describes the average properties of that particular surface. The product of this quantity σ° and the area contributing to a particular return signal can be thought of as the sum of the individual scattering coefficients σ_i as indicated in eq. (2). Thus, the differential scattering coefficient is defined by

$$\sigma^\circ = \frac{(4\pi)^3 R^4}{G^2 \lambda^2 \Delta A} \left(\frac{\overline{P}_r}{P_t}\right) \qquad (3)$$

In this equation, the gain and the wavelength are parameters of the radar. The range, R, is determined by the experiment being conducted and the area ΔA is jointly determined by radar and experiment. Evaluation of the differential scattering cross section involves measurement of the power ratio indicated and computation based on eq. (3).

If a pulse radar transmits a single pulse and the power received for that pulse is used in eq. (3), the quantity calculated is not σ°. For any <u>particular</u> position of the radar one must take into account the relative phases among the contributions from the different elements with cross sections σ_i. The average (indicated in the definition of both σ° and $\overline{P}_r$) involves measurements by moving the radar to a number of positions and consequently measurements made at a number of different times. The differential scattering cross section can only be calculated when enough measurements to compute a good average have been made at points where the signals are essentially independent of each other.

An illustration of the sort of fading encountered by a pulse system appears in Figure 10. The signal observed comes from a surface that stretches the pulse out. Hence, at intervals equal to the duration of the transmitted pulse, the signals come from different parts of the surface. Since they come from different parts of the surface, the phase combinations may be different. The result for several pulses measured in sequence is shown in the figure. The necessity for averaging is obvious!

3.2. MEASURED VARIATION OF σ°

Numerous measurement programs have attempted to define the differential scattering coefficient variations with terrain type and other parameters. The most complete and careful measurements are those of Ohio State University (Cosgriff, Peake, and Taylor, 1960) but unfortunately the size of the illuminated patch is only about a foot square, so these carefully measured data are not very representative of the areas likely to be encountered in scatterometry. These careful measurements at a fairly wide range of wavelengths and polarizations were made over numerous different kinds of micro-terrain. Furthermore, changes in return from specific plots were observed that were due to environmental changes, like crop growth and presence of rain and snow.

Airborne measurements are always difficult to correlate with adequate ground truth information. Observations over the land by Sandia Corporation (Edison, Moore, and Warner, 1960) made within 20° of the vertical had fairly good control of ground truth. Over a wider range of angles extensive radar measurements have been made without the ground truth information by the Naval Research Laboratory (Ament, Macdonald and Shewbridge, 1959). Measurements by the Goodyear Aircraft Corporation (Reitz, 1959) were intermediate in the amount of ground truth, but were made with a side-looking radar which permitted only a single angle of incidence for each target, so that curves of scattering cross section as a function of angle of incidence had to be made by identifying similar targets observed at different angles. Other measurement programs of this nature have been summarized in the monograph by Janza (1963).

Radar scatter measurements over the sea would appear to be easier because the "ground truth" need not be so detailed; the ocean's surface is statistically homogeneous over a distance of several miles if the measurements are far from a coastline and the dielectric properties of the surface are almost the same everywhere. Lack of good measurements of the sea state, however, make correlation of sea-state and radar measurements difficult. Measurements presently underway should greatly improve our knowledge of correlation between quantitative sea-state information and radar return. These measurements are coordinated by I. Katz of Applied Physics Laboratory with the radar measurements by F. C. Macdonald of Naval Research Laboratory and stereo photography of the sea by W. Marks of Oceanics, Inc.

Much of the previous information on correlation of sea-state with radar return has been compiled by Beckmann and Spizzichino (1963). The relationship between wind, wave height, and radar return indicated by this work is quite clear. Near vertical incidence, increasing wind and waves reduce the radar return. Near grazing incidence, increasing wind and waves increase the radar return. Beckmann and Spizzichino show a quantitative comparison for short wavelength data.

The conclusions of all of the experimental data are indicated in Figure 13 along with some interpretations based on theory. Relatively smooth surfaces, such as the ocean, give strong returns near the vertical that fall off rapidly with angle. Surfaces having the same geometry as the sea surface, but smaller reflection coefficients, such as deserts, have scattering coefficient curves with the same shape but smaller absolute magnitude. Surfaces rough compared with the wavelength, such as forests, or, for very short wavelengths, rough gravels, have smaller scattering coefficients near the vertical than the smoother surfaces, but their scatter changes little with angle so that near grazing, the return from the rough surface is much greater than that from the smooth surface. Both experimental observations and theory also indicate that returns near the vertical are due to larger scale fluctuations in the surface than the returns near grazing angle of incidence. Detailed curves for specific materials are given in the various references.

3.3. THEORETICAL VARIATION OF σ°

Theory of radar return from rough surfaces has received much attention in recent years because of the interest in interpreting radar returns from the moon. Scattering from the sea, however, has been studied longer and prompted one of the first treatments that successfully predicted at least a part of the radar backscatter (Davies, 1954). Davies cast the problem of scatter from the sea in terms of Huygens sources on the statistically described surface. Many other authors have used similar techniques with more refinements (see for example Hoffman, 1955; Moore, 1957; Hayre and Moore, 1961; Hagfors, 1961; Beckmann, 1965; Fung, 1965). Excellent summaries of the earlier work are contained in the book by Beckmann and Spizzichino (1963) and in Janza's monograph (1963). Similar techniques have been used for studying the scattering of acoustic waves from rough surfaces (see for example Eckart, 1953). A recent theoretical and modeling acoustic study is described by Parkins (1965).

Other theoretical work has been based on geometrical optics techniques using a model that describes the surface in terms of facets whose slopes (and sometimes size) are described statistically (see for example Muhleman, 1964). A modified geometrical optics method is necessary, however, when the surface is quite flat and we wish to know scatter for angles having no normally oriented facets (see Katzin, 1956, 1959). Other interesting approaches are due to Katz and Spetner (1960) and to Twersky (1957).

All of these theoretical studies depend upon a statistical description of the surface being observed. This is difficult for the sea and even more difficult for land surfaces that are covered with vegetation. Cosgriff, Peake, and Taylor (1960) have developed a theory for return from vegetation that may be represented by vertical cyclinders, but no theory for more complex shapes has been developed.

Most of the theories describe the surface in terms of an autocorrelation function of surface height vs. horizontal distance and assume a Gaussian distribution of surface heights. Simplified correlation functions have been used in the theoretical development because pertinent integrals are

intractible with more realistic correlation functions.

Few of the theoretical treatments take account of polarization differences. None of them takes into account the fact that the waves penetrate somewhat into any natural surface and that part of the signal returned may be due to irregularities beneath the surface rather than on it. Theoretical work on this problem is presently being started.

Although the theoretical calculations differ depending upon the surface model and upon the approximations used, they all agree reasonably well with Figure 11. Variation with wavelength, however, is not well established. Katz (1966) has studied this variation over rather wide ranges and concludes that different materials produce different scattering coefficient variations with wavelength. From grazing to within about 20° of the vertical, nearly all surfaces have differential scattering coefficient variations that increase with increasing frequency. Within about 20° of the vertical and certainly at the vertical itself, this variation is reversed; that is, lower frequencies give larger differential scattering coefficients. Katz shows that the manner of variation differs quite a bit among various surfaces, so that observation of the differential scattering coefficient over a wavelength range should help in using it to determine composition of a surface.

Variations with polarization are also different for different materials, so that comparison of returns from different polarizations may be useful in determining properties of materials. For the ocean, such polarization measurements may permit determination of the direction of waves.

3.4. SUMMARY OF PARAMETERS GOVERNING RADAR RETURNS

Variations in radar returns are due to certain parameters of the radar itself and to certain parameters of the surface being sensed. Parameters of the radar itself that are significant include:

angle of incidence

polarization

wavelength

The angle of incidence may vary over angles all the way from vertical to grazing. The strongest backscatter signals are observed for incidence near the vertical.

One may transmit either vertical polarization, horizontal polarization, or some combination--the usual combination is circular polarization. The signal may be received with the same polarization that was transmitted or with a different polarization or both.

Radar scatterometry is feasible with wavelengths from fractions of a micron (using lasers) to tens of meters. The normal range considered for radar scatterometers, however, is from a few millimeters to a few meters wavelength. This range is wider than that from violet light to the longest infra-red wavelength commonly in use.

Parameters of the surface that determine the radar return once the angle of incidence, polarization, and wavelength have been selected are:

roughness (described in wavelength units)

electrical conductivity

electrical permittivity

The roughness may be described either as the shape or as the texture of a surface; both are important.

Theories developed so far can only use relatively simple statistical descriptions of the surface. Natural surfaces, however, may be quite complicated and empirical comparison of surface qualities not readily described mathematically with radar return permits use of the scatterometer to identify surfaces, like forests, for which theory is inadequate.

Conductivity of the material is important in determining the amount of penetration. If the conductivity is high (as it is in sea water), it is a primary determinant, also of the reflection coefficient. If, on the other hand, the conductivity is low, the reflection coefficient in the radar wavelength region is established principally by the permittivity (dielectric constant). For most radar wavelengths the permittivity is more important than conductivity in determining signal strength (provided the medium is homogeneous to at least one skin depth -- the skin depth being determined by the conductivity).

As with visible and infra-red parts of the spectrum, theory is useful in determining what to expect and when to ask questions about experimental results. On the other hand, observations of

natural objects at these shorter wavelengths would indeed be in a sad state if one had to wait for development of adequate theories before using his eyes and before using infra-red sensors. The same is certainly true of radar wavelengths; that is, even for surfaces we cannot describe adequately with a mathematical model, empirical experimental determination of the radar return can be used to develop a catalog of signatures. Measurements currently underway by NASA Manned Spacecraft Center aircraft will provide some entries into this catalog. The Ohio State data provide others. The NRL measurements of sea-state will provide still others. As yet, however, the detailed catalog is far from complete.

Information available at this time conclusively demonstrates that significant variations with angle, polarization, and wavelength do exist, so that this technique can, in fact, be useful for sensing properties of the surface. A sound theoretical justification exists for using the scatterometer to measure ocean waves. The theoretical justification is more difficult with the more complicated surfaces but experiment indicates the usefulness there too.

4. FAN-BEAM RANGE-MEASURING SCATTEROMETER

Most scatterometer systems developed in the past for measuring radar cross section have used either broad antenna beams and depended entirely on range measurement or have used beams narrow in both dimensions like those of Figure 2a. Even narrow-beam systems, however, have often combined range measurements so that picture of Figure 2c is more appropriate. The fan-beam system has been proposed many times but has not often been used because most of the previous measurements were made with existing equipment designed for other purposes.

Although frequency-modulated radar altimeters have been in use for more than 25 years, most scatterometers use pulse modulation to measure range. Accordingly, most of the detail in this discussion refers to the pulse system.

The previous extensive use of pulse systems should not lead to the inference that these systems are necessarily the best for scatterometry. Rather, they have been used because they were the most available systems and special systems for scatterometry were not designed. In fact, either an FM system or a CW system may offer many advantages over the pulse system for scatterometer operation. A brief discussion of the FM system is included in this section. Limitations of time and space do not permit detailed treatment of the velocity measuring system, but for many purposes it may, in fact, be superior to the more commonly used systems discussed here.

4.1. DESCRIPTION OF PULSE SYSTEM

The operation of the pulsed scatterometer using a fan-beam was illustrated in Figure 9. Here the illuminated ground segments corresponding to angles from the vertical out to θ_4 are indicated. The radiated pulse first illuminates the circle at the vertical and then illuminates successive rings. Only a portion of each ring is illuminated because of the angular limitation caused by the antenna beam. The width of the illuminated ring is determined by the pulse duration of the radar.

A scatterometer system to be used for this type of operation is illustrated in Figure 12. The timing system provides pulses to the transmitter which turn the transmitter on for the pulse duration τ. It also provides delayed pulses to the gating system at times delayed from the start of the transmitter pulse by the right amount to permit observation at vertical incidence and at θ_1, θ_2, θ_3, and θ_4. In the notation of Figure 9 this means the delays are t_o, $t_o + t_1$, $t_o + t_2$ and so on. The transmitted signal goes to the ground and returns through the receiver to the gating system. Those portions of the received signal that are gated through to the output go to separate averaging systems, and the average outputs corresponding to each of the angles are sent to the data processing unit for collation. Some elements shown in the sketch need be present in the flight system. The receiver output could be recorded or telemetered, along with timing information, for ground processing. The gated outputs could be recorded sequentially or telemetered sequentially for ground averaging. The telemetry or recording bandwidth required, however, is greatest at the output of the receiver and decreases by orders of magnitude until the output of the averaging system is reached. Further processing should not reduce the bandwidth significantly. Hence, an airborne scatterometer should carry all elements through the averaging system if reduction in telemetry or recording rates is desirable.

The received signal due to a single transmitter pulse is illustrated in Figure 13a. A sample of the transmitter pulse will appear in the receiver if required, and may appear simply because it is too difficult to eliminate. No signal is received after the end of this sample transmitter pulse until t_o when the first signals start to come back from directly beneath the radar. Because of the geometry (illustrated later) times corresponding to equally spaced angles are spaced unequally so that the gate times are close together near the first return (t_1 is close to t_o) and they are further apart for later returns (as shown in the diagram).

The observed signal, like that of Figure 10, is jagged in appearance. The signals of Figure 10 would have appeared spread out much as those of Figure 13a if a fan-beam had been used. With a transmitter pulse duration τ, a new independently fading signal appears for every interval τ in the received pulse -- provided, of course, that the receiver bandwidth is sufficient. Since each point on the pulse corresponds to a randomly fading signal, and since σ° is an average of such signals, the return amplitudes at the various gate outputs for individual pulses are not meaningful but must be averaged. Thus, if the entire pulse is averaged, one would obtain the signal shown in Figure 13b. The system of Figure 12, however, will not provide such a continuous pulse, but rather will simply provide the amplitudes at the indicated times. A curve could, of course, be drawn through these points to produce the illustration of 13b.

Figure 14 illustrates the processing required to obtain curves of scattering coefficient vs. angle. Sketch 1 indicates the location of the video signal between two transmitted pulses. The time between pulses is P, the total duration of the signal is S. Sketch 2 indicates the output of the gating system for a single transmitted pulse and for 7 time gates. Gate A is for vertical incidence, gate G is for the maximum incident angle. Random variations about the mean curve can be seen.

The averaging system acts separately on each of the gate outputs. Thus, sketch 3 indicates its action on the output of gate A. $\overline{A}_1$ is the average output for N pulses. It is the average for the first ground segment to pass under the radar at normal incidence. $\overline{A}_2$ is the average for the second element to pass under the radar (vertical incidence). The other averages are also indicated up through the 7th element. Sketch 4 indicates the same sort of averages for gate B. $\overline{B}_1$ is the average return from a segment observed at the angle corresponding to B at the time when the radar is directly over the segment giving $\overline{A}_1$.

Since the outputs of the individual averaging circuits for any particular time correspond to different segments of ground, collation must be accomplished in the data processing. That is, $\overline{A}_1$ does not correspond to the same segment of ground as $\overline{B}_1$ or as $\overline{C}_1$. Preparation of a curve of scattering coefficient vs. angle for a particular section of ground must therefore wait until all the returns from that particular section of ground have been obtained and collated. Sketch 5 indicates this. If the fan-beam points ahead, a section of ground is first observed at the maximum incident angle. For this curve, we assume the first observation is in gate E and at time 2. As the radar advances toward the target segment, this segment is observed at the angle corresponding to gate D and the later time 4. Later, (at time 6) it is observed at gate C, still later (time 8) at gate B, and finally the radar passes directly over the ground segment at time 10 so that the output of gate A is appropriate. When these samples are all selected in the appropriate sequence and plotted as a function of angle of incidence, sketch 5 of Figure 14 results. A sequence of such plots, one for each ground segment, is obtained as the radar advances.

Because of variations in distance, illuminated area, and antenna gain, further computation must be performed on each of the values indicated in sketch 5 to produce a scattering coefficient as indicated in sketch 6.

Although this process is shown for the pulse system, outputs like those appearing in sketches 2 through 6 occur for any type of fan-beam scatterometer -- FM, PCM, or velocity measurement, so that the processing is similar for all system types.

4.2. GEOMETRY OF RESOLUTION

The ideal range-measurement fan-beam scatterometer would illuminate a constant-width strip along the flight path. Bands of constant thickness extending across this strip would be established at uniform angular intervals by the range measuring system. Figure 15a illustrates this. Idealized antenna patterns that have constant gain over a specified angular width and zero gain outside of that are frequently used in discussing radar and other systems. Figure 15b shows the pattern of ground illumination caused by such an ideal antenna pattern with a fan-beam.

In reality, of course, neither the ideal ground illumination nor the ideal fan-beam can be achieved. Figure 15c illustrates a more realistic ground illumination with a fan-beam. The antenna is pointed with its maximum in the direction indicated for the maximum gain contour. The pattern, instead of having straight iso-gain lines on the ground, has a rounded contour. Furthermore, the gain falls off gradually rather than dropping suddenly to zero. Figure 15d shows cross-sections of the pattern of 15c. The dash lines indicate the idealized rectangular patterns shown in Figure 15b and the solid lines are the actual patterns. Thus, one can sketch contours of constant gain on the ground as in Figure 15c. It is customary to use the half-power contour to describe the illumination of a particular antenna, although for some purposes the 1/10 power contour might be more appropriate. In the discussion that follows a pattern like that of Figure 15b is assumed, but only for simplicity of analysis.

Pulse length limitation of illumination with relatively wide antenna beams is indicated in Figure 16. The beams are assumed to be idealized and conical in shape with uniform gain out to the limits of illumination and no gain beyond that. They are assumed pointed straight down as they might be for a scatterometer that looks both ahead and behind. R_2 is the slant range to the position of the leading edge of the pulse, h is the altitude and R_1 is the slant range to the trailing edge of the pulse. The angles Θ_2 and Θ_1 correspond with R_2 and R_1. Corresponding ground distances are ρ_2 and ρ_1.

Figure 16a shows the situation before the trailing edge of the pulse has hit the ground. Thus,

$$R_2 < h + \frac{c\tau}{2} .$$

The limits of the pulse illumination are spheres centered on the radar. Figure 16a shows an illuminated region that is a circle directly under the antenna. Figure 16b shows the situation when the trailing edge has hit the ground but the leading edge is still within the area permitted by the antenna to be illuminated. The illumination, then, is a ring. Later on (not shown) the leading edge goes beyond the limits of the antenna beam and the ring decreases in width until the trailing edge hits the limit of the antenna beam after which no signal returns. Analysis in detail is given later. Figure 16c is an expanded view for relatively short pulses at angles such that are R_1 and R_2 may be considered parallel. The width of the ring is indicated here as $\Delta\rho$ which is clearly given by

$$\Delta\rho = \frac{c\tau}{2\sin\Theta}$$

The average pulse shape generated for constant σ° under these conditions is shown in Figure 16d. There is a linear build-up of return power until the trailing edge hits the ground. The slow decay occurs because of the increasing range and slightly decreasing area of the illuminated region. The more rapid decay is caused by passing of the area permitted by the pulse length to be illuminated outside that permitted by the beamwidth to be illuminated. When σ° falls off with angle, the build-up is not quite linear and the decay is more rapid.

A narrow-beam system looking straight down with a relatively long pulse would be beamwidth limited rather than pulse-length limited. The illuminated area starts off as a circle as shown in Figure 17a. The circle radius increases until it is equal to the radius of the beam intersection with the ground. When the trailing edge hits the ground, the circle becomes a ring decreasing in width. During the interval after the leading edge has filled the beam and before the trailing edge has hit the ground, the mean return signal is constant. This situation is indicated in Figure 17c.

Figure 17d indicates the way the beamwidth limits the illumination for a fan-beam system (or any other system in which the beam is pointed away from the vertical). For a beamwidth β, the radar illuminates a width b on the ground. Thus,

$$b \approx R\beta \tag{4}$$

Figure 18 details the geometry for an idealized fan-beam scatterometer. The fan-beam antenna is pointed at an angle γ from the vertical in the direction OB. The axis of the antenna that passes through a vertical plane is OG. The beam-width of the antenna is the angle AOC. The limits of the beam for the idealized antenna are the planes intersecting in the line OG and passing through OA and OC. The intersection of these planes with the ground is given by GDAH and GFCJ. Let us define the width of the beam on the ground as b, with b_a the width at the pointing angle (AC) and b_o the width at vertical incidence (DF). Using these definitions and the geometry indicated in the figure we find

$$\frac{b_o}{b_a} = \frac{DF}{AC} = \cos^2\gamma \tag{5}$$

If the angle AOC and the angle DOF were the same, this ratio would be only $\cos\gamma$. The additional reduction in b_o is due to the angle made by the plane DOFE with the line OG.

The general expression for the width illuminated can be shown to be

$$\frac{b}{b_a} = \frac{HJ}{AC} = \cos^2\gamma\,(1 + \tan\Theta\,\tan\gamma) \tag{6}$$

This is somewhat more compact when expressed in terms of b_o as

$$\frac{b}{b_o} = 1 + \tan\theta\tan\gamma \tag{7}$$

The variation of the width of the illuminated area with angle of incidence for various pointing angles is shown in Figure 19. It is apparent that the increase in width beyond about 60° is so rapid that attempts to use the scatterometer beyond this incident angle are bound to result in excessively wide ground segments.

The resolution distance along the flight axis is determined by the pulse length. The difference in slant ranges between the leading and trailing edge of the illuminated area is $c\tau/2$. Writing the slant ranges in terms of the height and the angle, this results in

$$\frac{c\tau}{2} = R_2 - R_1 = h\left(\frac{1}{\cos\theta_2} - \frac{1}{\cos\theta_1}\right) \tag{8}$$

For most purposes a more meaningful set of angles for the segment than the inner and outer angle is the average angle and the difference in angle. We define the average angle as

$$\theta_m = \frac{\theta_1 + \theta_2}{2}$$

and the angular difference as

$$\Delta\theta = \theta_2 - \theta_1$$

The expression for the angular width then appears, after considerable algebraic manipulation, as

$$\sin\frac{\Delta\theta}{2} = \frac{\sin\theta_m}{\left(\frac{c\tau}{2h}\right)}\left[\sqrt{1 + \left(\frac{c\tau}{2h}\right)^2 \cot^2\theta_m} - 1\right] \tag{9}$$

This expression applies only for angles large enough so the trailing edge of the pulse has hit the ground; that is, when

$$\theta_m \geq \frac{\theta_2}{2}$$

The condition for this can be shown to be

$$\cos\theta_2 = \frac{1}{1 + \frac{c\tau}{2h}} \tag{10}$$

Except very close to this limit the second term under the square root in eq. (9) is small compared with unity and eq. (9) may be approximated by

$$\Delta\theta \approx \left(\frac{c\tau}{2h}\right)\cos\theta_m\cot\theta_m \tag{11}$$

The limiting case at the vertical is given by

$$\sin(\Delta\theta) \approx \sqrt{\frac{c\tau}{h}} \tag{12}$$

Clearly the shape of the curve of variation of $\Delta\theta$ is the same for all pulse lengths. However, the ratio $(c\tau/2h)$ is a scale factor. The expression of eq. (12) determines the minimum angle and is itself determined by $(c\tau/2h)$. Figure 20 illustrates this variation in resolution angle with incidence angle for two cases: (1) where height is 50 times the pulse length in space and (2) where it is 250 times the pulse length in space. Although the minimum θ_m for the first ratio is 8°, the $\Delta\theta$ falls off very quickly to less than 1°. When the altitude is 5 times as many pulse lengths, the minimum angle is smaller (3.60°) and the difference angle is quite small indeed even at relatively low incident angles.

The width along the ground is usually a more significant parameter than the angular width. Fundamentally it is given by

$$\Delta\rho = R_2 \sin\theta_2 - R_1 \sin\theta_1 \tag{13}$$

Substituting for θ_2 and θ_1

$$\theta_2 = \theta_m + \frac{\Delta\theta}{2}$$

$$\theta_1 = \theta_m - \frac{\Delta\theta}{2} \quad , \tag{14}$$

and performing considerable manipulation give for the expression for the width on the ground for $c\tau/2h << 1$

$$\Delta\rho \approx \frac{c\tau}{2\sin\theta_m} \left(1 + \frac{c\tau}{2h} \cos^3\theta_m\right) \tag{15}$$

It is interesting to note that this is approximately equal to the approximate expression derived from Figure 16c.

This expression also is limited to the situation where the complete pulse illuminates the ground. This limiting maximum value for $\Delta\rho$ is given by

$$\Delta\rho \approx \sqrt{c\tau h} \tag{16}$$

A major difficulty for range measurement scatterometers is the presence of the square root near the vertical. The pulse must be shortened by a factor of a hundred to reduce the illuminated width by a factor of ten. Usually shortening a pulse by a factor of a hundred is not feasible.

Expressions for the width on the ground transverse to the flight track given in eq. (4), (6), and (7) may be combined with the expression for the length along the track of eq. (15) and (16) to compute the size of the resolvable segment of the ground. An example serves to illustrate the parameters that a practical scatterometer might encounter.

Let us assume a beamwidth of .05 radians, an altitude of 2000 meters, an antenna pointed at 30° from the vertical and a pulse length of 0.1μs. Summarizing:

$$\beta = 0.05 \text{ radians}$$
$$h = 2 \cdot 10^3 \text{ m}$$
$$\gamma = 30°$$
$$\tau = 0.1\mu s$$

At the 30° pointing angle we find $b_a = 115$ meters. At the vertical $b_o = 86.6$ meters, and at 60° $b_{60°} = 173.2$ meters. With the assumed pulse length and altitude we have the following set of angular widths:

$$\Delta\theta_o = 7.0°$$
$$\Delta\theta_{30°} = 0.65°$$
$$\Delta\theta_{60°} = 0.125°$$

With these go the following widths along the ground:

$$\Delta\rho_o = 245 \text{ m}$$
$$\Delta\rho_{30°} = 30 \text{ m}$$
$$\Delta\rho_{60°} = 17.3 \text{ m}$$

Thus, the illuminated segment at the vertical is (from vertical out) 245 m by 86.6 m . At 30° it is 30 m by 115 m, and at 60° it is 17.3 m by 173.2 m . These widths are rather large, but a narrower antenna beam that would be feasible if the wavelength were short enough would reduce the width across track. The variation between the vertical and 60° in the along-track width is characteristic of the range measurement scatterometer. As shown in Section 4.3 the short length at 60° is not especially meaningful, as the effective distance in that direction at that angle will be greater.

4.3. FADING RATE LIMITATIONS

Averaging to get meaningful values for σ° requires the signal to be observed long enough that sufficient independent samples may be collected. Independent samples may arise from two causes: independence within the Doppler fading spectrum while illuminating a single ground patch from different angles and combination of returns measured from completely separate ground patches. Often it is necessary to combine these effects to get enough independent samples.

The difference in Doppler frequency between the inner and outer extremes of an illuminated region is given by

$$\Delta f_d = \frac{2v}{\lambda} \cdot \left[\left(\frac{R_2}{R_2} \right) - \left(\frac{R_1}{R_1} \right) \right] \tag{17}$$

This determines the total width of the Doppler spectrum to be observed. Since the elements in the return from different ranges have different relative velocities, and the phases are essentially random because of the locations of the scattering elements, a noise-like spectrum is produced by the fading. This spectrum must be studied to determine the independent sample rate.

Figure 21 shows a Doppler spectrum with Δf_d displaced above the carrier frequency f_c because of motions toward the target. The spectrum would be flat if the scattering coefficient and the range were constant from one side of the patch to the other; it may be considered essentially flat here. Figure 21b shows the spectrum after detection by a square law detector. The rectangular pre-detection spectrum is converted into a triangular spectrum extending to twice the width of the pre-detection spectrum.

The autocorrelation function associated with this spectrum may be computed. From this, an estimate of the time between independent samples may be made. The autocorrelation function is the one-sided Fourier cosine transform of the triangular spectrum of Figure 21b. It can be shown that this is

$$a(t) = 2 \frac{(1 - \cos 2\omega_d t)}{(2\omega_d t)^2}$$

Here $\omega_d = 2\pi \Delta f_d$. The amount of decorrelation necessary for independence is somewhat arbitrary. If we assume independence when the correlation function goes to zero and its envelope to $1/\pi^2$ (about 0.1) the time between independent samples is given by

$$t = \frac{1}{4\Delta f_d} = \frac{t_d}{4} \tag{18}$$

where

$$t_d = \frac{1}{\Delta f_d} \cdot$$

Thus, t_d is the period corresponding with the width of the pre-detection spectrum and the decorrelation time is one-fourth this period or half the period of the width of the post-detection spectrum.

Using this definition for the spacing between independent samples, the number of independent samples occuring during the time for the radar to pass a resolution element of width $\Delta\rho$ is given by

$$n_i = \frac{\text{time to traverse } \Delta\rho}{\text{time/sample}} \tag{19}$$

Thus,

$$n_i = \frac{\Delta\rho / v}{t_d / 4} = \frac{4\Delta\rho \Delta f_d}{v}$$

Substituting values found previously, this can be expressed as

$$n_i = \frac{8(\Delta\rho)^2 \cos^3 \theta_m}{\lambda h} \tag{20}$$

in terms of $\Delta\rho$, or as

$$n_i = \frac{2(c\tau)^2 \cot^2 \theta_m \cos \theta_m}{\lambda h} \tag{21}$$

in terms of τ.

Equations (20) and (21) show that the number of independent samples per ground segment is greater near the vertical than near grazing even if the width of the segment is the same. This comes about because the difference in angle between the extremes of the segment is smaller for angles nearer grazing so the difference in Doppler frequencies is smaller. Furthermore, since the Doppler frequencies are proportional to the sine of the angle and since the sine curve is flatter near $\pi/2$, the reduction in number of independent samples is magnified near grazing incidence. Since $\Delta\rho$ itself is smaller near grazing incidence, (21) shows an even greater variation.

To see what this means, consider its influence on the example quoted previously. The wavelength must be assumed and all other assumptions are the same. Let the wavelength be 10 cm. With this assumption eq. (21) yields 2400 independent samples at vertical, 23 independent samples at 30°, and only 1.125 independent samples at 60° ! From this it is obvious that at the larger angles several resolution lengths ($\Delta\rho$) must be used to obtain an adequate sample. For example, if the 245 m $\Delta\rho$ for the vertical is used at 30° and 60° the number of independent samples changes to 2400, 188, and 16.

The number of independent samples from the combination of several samples in passing across one resolution cell (described above) and examining returns from several independent resolution cells may be expressed by multiplying the results of eq. (20) or (21) by the ratio of total distance traversed to $\Delta\rho$. Thus, eq. (20) becomes

$$n_i = \frac{8(\Delta\rho)^2\cos^3\theta_m}{\lambda h}\left(\frac{L}{\Delta\rho}\right) = \frac{8L\Delta\rho\cos^3\theta_m}{\lambda h} \tag{22}$$

where L is the total distance travelled during calculation of an average. Eq. (21) becomes

$$n_i = \frac{4Lc\tau\cos^2\theta_m\cot\theta_m}{\lambda h} \tag{23}$$

Figure 22 illustrates this.

The number of independent samples required depends upon the accuracy desired. Of course, if the distance required to obtain enough independent samples is greater than the distance over which a terrain segment is homogeneous, a poorer accuracy must be accepted.

The noise-like characteristics of the return signal result in fading that follows a Rayleigh distribution. This distribution is characterized by equal mean and standard deviation; that is, the distribution after square law detection is given by

$$p(w) = \frac{1}{w_o}\, e^{-w/w_o}$$

$$\sigma = \mu = w_o \tag{24}$$

Here μ is the mean, w is the post-detection voltage, and σ is the standard deviation.

For relatively small numbers of independent samples, the standard deviation for the mean of Rayleigh distributed variables differs somewhat from that for normally distributed variables. As the number of samples increases, the central limit theorem applies and Rayleigh and normal results are very close. The standard deviation of the mean is given approximately by

$$\sigma_m = \frac{\sigma}{\sqrt{n}} = \frac{w_o}{\sqrt{n}} \tag{25}$$

For n larger than 20 or so, this approximation is quite good. For smaller values of n it is off both because of the necessity to apply small sample theory and because of the difference between the Rayleigh distribution and the Gaussian.

The 5% to 95% range that the mean can take on is given by

$$\text{Range} = 2 \times 1.645\sigma_m = \frac{3.29\mu}{\sqrt{n}} \tag{26}$$

when the assumptions of eq. (25) are made. Expressed in decibels this range is plotted in Figure 23. Clearly, a range of 2 to 3 db is easy to achieve, but a range much better than 1 db requires a very large number of independent samples and consequently a large $\Delta\rho$. Experiment design must take this into account, and compromise is necessary between the maximum allowed $\Delta\rho$ and the desired range for the mean value.

4.4. DYNAMIC RANGE PROBLEMS

The dynamic range required for the receiver in a radar scatterometer operating between vertical and 60° is so great that it is extremely difficult to achieve with a linear system. With a logarithmic system, it is not difficult. The worst situation for dynamic range is the return from relatively smooth targets, like calm sea.

The scattering coefficient σ° for a smooth sea may vary from 30db at vertical incidence to less than -30db at 60°. Thus, even if all signals returned were of the mean value, a dynamic range of 60db would be required for a receiver covering the total range of angles. Over the land the situation is not so bad. +10db is a relatively high value for σ° over land although occasionally it gets higher. An area with such value at the vertical would probably have a σ° no lower than a -25db at 60°. Thus, a 35db range is indicated.

The dynamic range of the system must take into account not only variation in σ° but also the fading about this value. The 5% to 95% range for a Rayleigh distribution is 18db (+8db to -10db). Thus, the receiver must be able to accomodate from +38db to -40db if it is to cover that range for the smooth sea example or from +18db to -35db for the land example. The total ranges indicated are respectively 78db and 53db.

The wide dynamic range can be accomodated in various ways. Four possible solutions are:

1. Use of logarithmic IF amplifier.
2. Variation of receiver gain with range in accordance with some standard curve.
3. Stepping the gain of the receiver for different ranges.
4. Use of separate receiver channels for different angular regions.

Scatterometers that operate over a fairly narrow range of angles do not have dynamic range problems to the same extent as those operating over a wide range of angles; but a scatterometer operating near the vertical has to handle a quite wide dynamic range even if it only goes out to about 20°, for the curves of σ° vs. θ are often quite steep near the vertical.

4.5. SENSITIVITY CALIBRATION

Calibration of the absolute sensitivity of a radar set is difficult because so many different factors must be considered. Fortunately, many of the applications of scatterometry depend upon the shape of the curve of scattering coefficient vs. angle rather than upon accurate measurements of its level. Relative calibrations are easier to make than absolute calibrations.

The best calibration system for a scatterometer is one based upon an actual radar measurement. Such a calibration takes into account with one measurement variations in transmitter power, antenna gain, microwave transmission losses, receiver sensitivity, and receiver output calibration. The Naval Research Laboratory has for some time calibrated by using the radar return from spheres dropped behind the aircraft. Since a metallic sphere has a cross section that may readily be calculated theoretically, and the agreement between measurements and theoretical calculations is good for spheres, this is a satisfactory system, except that the spheres are lost and must be tracked as they fall.

Another technique that is harder to apply, but that can be used occasionally, is measurement of the return at vertical incidence from smooth water. Since all water has essentially the same dielectric constant and since at most radar frequencies the conductivity does not determine the reflection coefficient, the specular reflection from any patch of smooth water should be identical with that from any other patch of smooth water. The trouble with this system is that smooth water is hard to find. For calibration purposes, the water must be sufficiently smooth that the radar signal does not fade very much. If, instead of the 18db 5% to 95% range for a Rayleigh distribution, a fading range of 3db or 4db is observed, the water may be smooth enough for calibration purposes.

When known calibration targets like spheres or smooth water cannot be used, a calibration system is desirable that sends signals as much as possible like the received signals through as much of the radar system as possible. The most desirable approach would be to send a sample of the transmitted signal through the receiver from a point as close to the antenna as possible. Unfortunately, with pulse systems the transmitter usually couples enough energy into the receiver to saturate the receiver unless extreme measures are taken to protect the front end of the receiver. Because of these measures, the sample that gets through is far from representative and not usable for calibration. Samples have been transmitted through the receiver after delaying them in a long delay line, but such delay lines are bulky.

If a transmitter sample cannot be used in the receiver, a pulsed signal generator should be fed into the receiver near the antenna and a measurement should also be made of the transmitted power.

Such a system is subject to errors as indicated by Janza (1963). Careful calibration, however, permits an absolute accuracy somewhere between ± 1db and ± 3 db.

4.6. FREQUENCY MODULATED SYSTEMS

Frequency modulation is, except for pulse modulation, the most widely used range discrimination system. For simplified analysis it is common to consider a system in which the frequency sweeps linearly from some unspecified minimum to an unspecified maximum as indicated in Figure 24a. In fact, however, a limit must be specified on the range of the sweep and this introduces additional complications.

The fundamental FM principle is illustrated by Figure 24. Figure 24a shows variation of frequency with time. The transmitted frequency, f_t, increases linearly with time. The signal from directly beneath the radar returns with the minimum time delay t_h. It is, therefore, at the frequency that was being transmitted a time, t_h, earlier. The difference between that frequency and the one being transmitted when it is received is f_s. f_s may also take on other values for signals returned from larger ranges. Thus the dash line in the figure shows the longer time delay associated with a longer range. The four f_s lines show the received signal from four different ranges.

In Figure 24b the spectrum of signals received is shown. The maximum signal, of course, is received from the shortest range and has the lowest f_s. Signals received from longer ranges have larger frequencies associated with them. This curve should be compared with the analogous pulse shape of Figure 13.

Figure 25a shows the way transmitted and received frequencies vary for a target at a single range with a saw-tooth modulation. The single frequency corresponding to one element of the spectrum of Figure 24b is the horizontal line in Figure 25a. Of course, additional frequencies are introduced by the cross-over between increasing and decreasing frequency modulation.

Because the Doppler effect causes a frequency shift, its effect on FM system performance exceeds its effect on pulse system performance since the range and velocity are both measured by frequencies in the FM system. Figure 25b shows what happens when the Doppler frequency is positive (again for a single target). The average frequency of the plot at the bottom is the same as without Doppler frequency, but on individual sweeps the signal frequency is shifted either up or down. If the Doppler frequency is relatively small, this merely amounts to broadening of a given spectral line. If it is large, separate filters must be used for the upper and lower frequencies. In fact, it is possible for the Doppler frequency to be larger than the signal frequency, in which case the signal frequency appears as a modulation on a Doppler frequency sub-carrier.

The basic frequency modulated scatterometer system is shown in Figure 26. The mixer combines a sample of the transmitted signal with the signal being received. Its output is the difference frequency f_s. This is amplified and passed through separate filters corresponding to the different ranges and, consequently, different angles. The filter outputs are averaged and either recorded or displayed. Numerous variations are possible in this system. For example, a super-heterodyne system can be constructed, and the filtering might be done either at the intermediate frequency or after a second mixer. Signal-to-noise performance can be improved by introducing a low-noise amplifier between the receiving antenna and the mixer. Various modulation schemes other than the saw-tooth shown are also possible. The fundamental relations governing the system of Figure 24 are

$$f_t = f_c + mt$$
$$f_r = f_c + m\left(t - \frac{2R}{c}\right)$$
$$f_s = \frac{2R}{c}m \tag{26}$$

Here, m is the modulation rate and R is the general slant range. If the width of a filter is Δf_s, this means that it is related to a range difference and to a resolution width by

$$\Delta f_s = \frac{2m\Delta R}{c} = \frac{2m\Delta\rho \sin\theta_m}{c} \tag{27}$$

The equivalent pulse width is, of course, given by $\Delta R = \frac{c\tau}{2}$. Hence,

$$\Delta f_s = m\tau \tag{28}$$

By using this equivalent pulse length, the computations of Section 4.2 can be used to determine resolution variations.

The effect of finite sweep frequency width and of Doppler shift complicates these analyses so much that this effect will not be treated in detail here. The finite repetitive sweep changes the continuous spectrum of Figure 24b into a discrete spectrum and tends to smear it somewhat, the amount of smearing depending upon the sweep rate and total width. Various systems primarily for use against single targets rather than against the ground have been developed that take advantage of the spectral lines by using narrow filters to enhance signal-to-noise ratio.

Averaging of independent samples comes about differently with the FM system than with the pulse system. The Doppler shift from one end to the other of the ground segment observed is the only means for obtaining the various elements of the fading pattern and, consequently of the Rayleigh distribution, with the pulse system. With the FM system, the sweep in frequency may pass through peaks and nulls of the diffraction pattern of the scattering ground surface just as travel in distance passes through peaks and nulls and results in the Doppler shift. Hence, some averaging may occur in a single sweep and the time between independent samples may be determined by the width of the filter that sets ground resolution rather than by a Doppler effect. Calculations shown here neglect the Doppler effect, on the assumption that m is selected so as to make Doppler shift negligible. This is possible with relatively low speed aircraft, but with jet aircraft and spacecraft, a more complicated analysis must be made.

Considering the same autocorrelation analysis as in Section 4.3 the time for independent samples is one-fourth the period corresponding to the spectral width of the filter provided that square law detection follows the filter output. That is,

$$t_i = \frac{t_d}{4} = \frac{1}{4m\tau} .$$

Using this relation in eq. (19) the expression for the number of independent samples in the idealized FM case is

$$n_i = \frac{4\Delta f_s \Delta\rho}{v} = \frac{8m(\Delta\rho)^2 \sin\theta_m}{cv} \tag{29}$$

In fact, the idealized situation does not occur, although it may be approximated if the frequency deviation is great enough. In Figure 25, consider the duration of the single sweep to be T. The total frequency deviation is

$$F = mT .$$

If the time between independent samples is the same as calculated before (and it may not be if it is too small compared with T) the total number of independent samples obtained during one sweep is given by

$$n_i = \frac{T}{t_i} = 4m\tau T = 4F\tau \tag{30}$$

If n_i is small, the factor of 4 is certainly in error. The best possible resolution that can be obtained with a system having deviation F corresponds with a time delay τ. Hence, in order to get very many independent samples within a sweep, the time τ must be considerably longer than the minimum that could be used with the given deviation.

If the deviation is large enough and the sweep is slow enough, the analysis above holds. If, however, the deviation is sufficiently small that the product $F\tau$ is close to unity, the spectrum of the periodic waves is vastly different from that for the aperiodic wave of Figure 24a. Furthermore, the effect of Doppler can be quite severe. If the Doppler frequencies are such that the time between independent samples due to Doppler fading is considerably greater than that for the FM system, the effect of the Doppler fading is simply the same as in the pulse system but with n_i of eq. (30) as a multiplier. This implies that the Doppler frequency shifts are only a small percentage of the bandwidth of the filter used in the FM system. If the Doppler frequency shift is a significant percentage of this filter bandwidth, not only the analysis but the system must be changed.

An example to illustrate the application of these can be made similar to the example of Sections 4.2 and 4.3. In this case, we must also specify the frequency modulation parameters. Let us assume 100 mc deviation and a sweep duration of 10^{-2} sec. As with the previous example, we assume $\tau = 10^{-7}$ seconds, $v = 200$ m/sec , $\lambda = 0.1$ m . Applying eq. (30) we find that $n_i = 40$; that is, in one sweep there are 40 independent samples because of the deviation in frequency. This

method can be used provided the time for independent samples due to Doppler frequency is long compared with the time for independent samples due to sweeping. This is, indeed, the case as the time between independent samples for sweeping is 0.25 ms while that for Doppler shift is 7.25 ms. If we had assumed a frequency deviation of only 10 mc instead of 100 mc, the situation would have been greatly different.

5. DATA PRESENTATION

Scatterometer outputs are in the form of curves of scattering coefficient vs. angle. Sets of these curves must frequently be presented simultaneously because the scatterometer operates with different wavelengths and different polarizations. Interpretation of such sets of curves is difficult without an improved presentation.

Since each scatterometer output must be related to a particular section of terrain, the first method that suggests itself for scatterometer presentation is to plot curves over a map for the region investigated. This is shown in the upper left-hand diagram of Figure 27 for a two-frequency (or two-polarization) scatterometer. Although this presents the information in its proper geographical context, it is still difficult to relate the various curves in any very easy manner.

The number of parameters associated with any one curve of σ° vs. θ is not known. Most of the simpler theories use only two parameters, but they do not fit experimental observations over a very wide range of angles. Other theories due to Katz and Spetner and to Fung and Moore, show how larger numbers of parameters may become involved, up to perhaps 5 for each curve. Quantizing of the curves to present these particular parameters may permit presentation modes that are easier to understand. The next sketch in Figure 27 illustrates one way of showing these quantized parameters. A color code may be assigned to replace curve shapes. Presentation would then appear as shown, where the different kinds of hatching represent different colors.

The number of quantities that may be conveniently presented with color is somewhat limited. If we combine color and the length of the bar as shown in the upper right-hand corner in Figure 27, the number of distinguishable combinations may be increased.

Other possibilities exist that offer promise of showing even more distinctions. For example, the lower left-hand corner of Figure 27 uses the color coding of the upper center, the length coding of the upper right, and adds to it width coding and angle coding. Thus, four different variables may be represented by separate quantities: color, length, width, and angle.

For many geoscience parameters, contours should be plotted to compare with, for example, height contours. For this purpose, multiple passes of the scatterometer are necessary. In the lower center of Figure 27 the color coding of the upper center is shown used to produce contours.

With the various combinations illustrated in the lower left-hand side of the figure different contours associated with different parameters may be plotted. The lower right-hand side shows a set of these contours, with color contours going one way and length contours another.

The illustrations of Figure 27 are only a first attempt at showing means to present scatterometer data. As more information becomes available from scatterometers these and other means of presentation will be tried to determine the ones that are most suitable for geoscience application.

6. REFERENCES

Ament, W., F. Macdonald, and R. Shewbridge. "Radar Terrain Reflections for Several Polarizations and Frequencies," Trans. 1959 Symposium on Radar Return, Part 2, May 11-12, 1959, (University of New Mexico), NOTS Technical Publication 2339, Naval Ordinance Test Station, China Lake, Calif.

Beckmann, P. "Scattering by Composite Rough Surfaces," Proc. IEEE, vol. 53, no. 8, August 1965, pp. 1012-1015.

Beckmann, P. and A. Spizzichino. The Scattering of Electromagnetic Waves from Rough Surfaces, The MacMillan Co., New York, 1963.

Cosgriff, R. F., W. H. Peake, and R. C. Taylor. "Terrain Scattering Properties for Sensor System Design, Terrain Handbook II," Engr. Exp. Sta., Ohio State University, Columbus, May 1960.

Davies, H. "The Reflection of Electromagnetic Waves from a Rough Surface," Proc. IEE, Part III, vol. 101, 1954, pp. 209-214.

Eckart, C. "The Scattering of Sound from the Sea Surface," J. Acoust. Soc. Am., vol. 25, 1953, pp. 566-570.

Edison, A. R., R. K. Moore, and B. D. Warner. "Radar Terrain Return Measured at Near-Vertical Incidence," Trans. IRE, vol. AP-8, 1960, pp. 246-254.

Fung, A. K. "Scattering Theories and Radar Return," CRES Report 48-3, University of Kansas, Lawrence, May 1965 (dissertation).

Hagfors, T. "Some Properties of Radio Waves Reflected from the Moon and Their Relation to the Lunar Surface," J. Geophys. Res., vol. 66, March 1961, pp. 777-785.

Hayre, H. S. and R. K. Moore. "Theoretical Scattering Coefficients for Near-Vertical Incidence from Contour Maps," J. Res. NBS D. Radio Propagation, vol. 65-D, 1961, pp. 427-432.

Hoffman, W. C. "Backscatter from Perfectly Conducting Doubly-trochoidal and Doubly-sinusoidal," Trans. IRE, vol. AP-3, 1955, p. 96.

Janza, F. J. "The Analysis of Pulsed Radar Acquisition System and a Comparison at Analytical Models for Describing Land and Water Radar Return Phenomena," Sandia Corp. Monograph SCR-533, 1963.

Katz, I. "Wavelength Dependence of the Radar Reflectivity of the Earth and the Moon," J. Geophys. Res., vol. 71, no. 2, Jan. 15, 1966.

Katz, I. and L. M. Spetner. "Two Statistical Models for Radar Terrain Return," IRE Trans. PGAP, vol. AP-8, no. 3, May 1960, pp. 242-246.

Katzin, M. "Sea Clutter at High Depression Angles with Applications to the Ground Clutter Problem," Radar Return Symposium, May 1959, NOTS TP 2338, U. S. Naval Ordnance Test Station.

Katzin, M. "Recent Developments in the Theory of Sea Clutter," IRE Convention Record, Part I, 1956, p. 19.

Moore, R. K. "Resolution of Vertical Incidence Radar Return into Random and Specular Components," Univ. of New Mexico, Albuquerque, Engr. Exp. Sta. Tech. Report EE-6, July 1957 (also Sandia Corp. Report SCR-6).

Muhleman, D. O. "Radar Scattering from Venus and the Moon," Astronomical J., Feb. 1964.

Parkins, B. E. "The Omnidirectional Scattering of Acoustic Waves from Rough Surfaces with Application to Electromagnetic Scattering," CRES Report 48-4, University of Kansas, Lawrence, June 1965 (dissertation).

Reitz, E. A. "Radar Terrain Study: Measurements of Terrain Backscattering Coefficients with an Airborne X-Band Radar," Goodyear Aircraft Corp., Litchfield Park, Ariz., Gera-463, Sept. 1959.

Twersky, V. "On Scattering and Reflection of Electromagnetic Waves by Rough Surfaces," IRE Trans. on Antennas and Propagation, vol. AP-5, Jan. 1957, pp. 81-90.

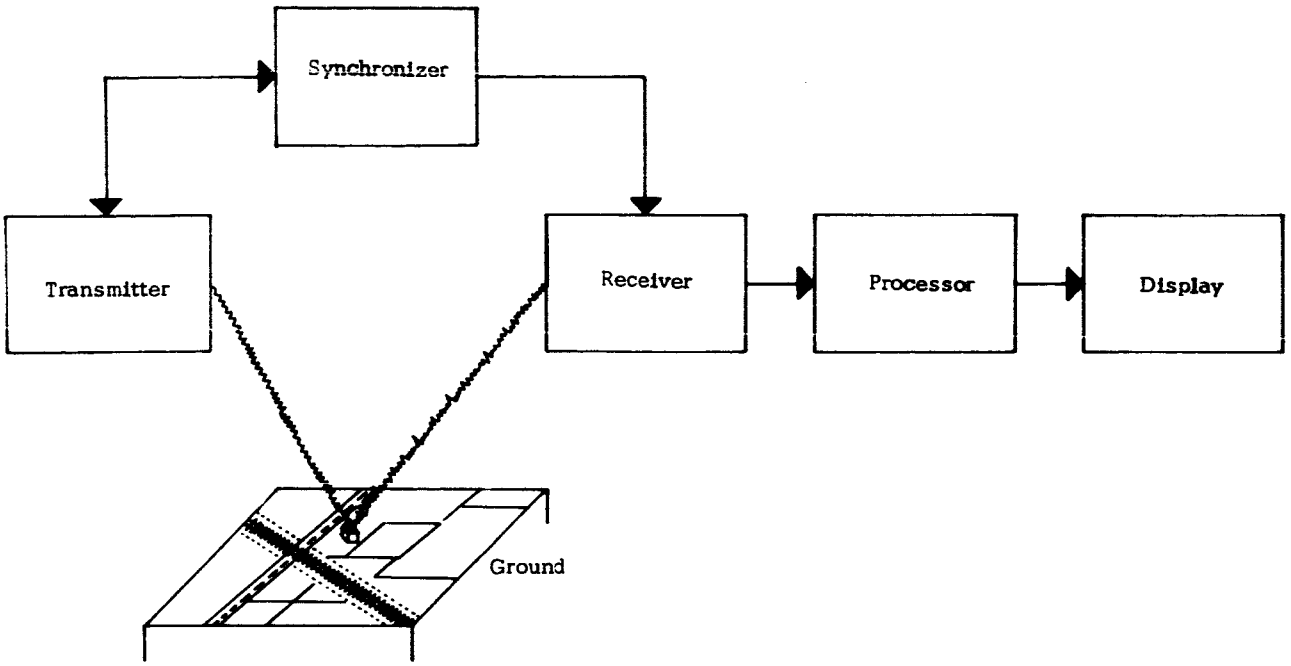

FIGURE 1. Elements of a Radar System

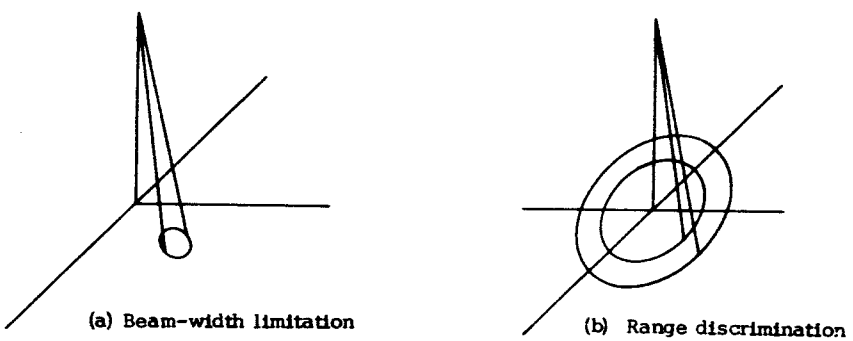

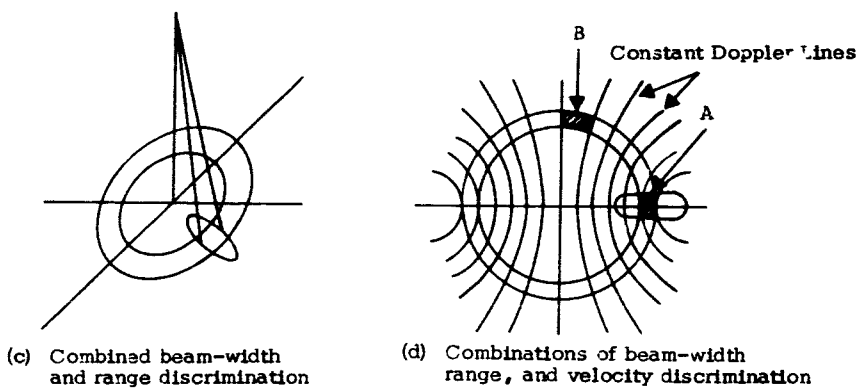

FIGURE 2. Discrimination Techniques for Radar

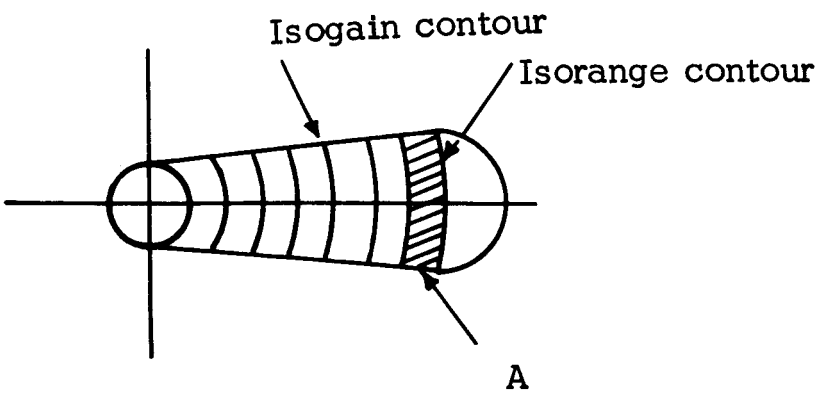

FIGURE 3. Angle-Range-Measurement Scatterometer Illuminated Region

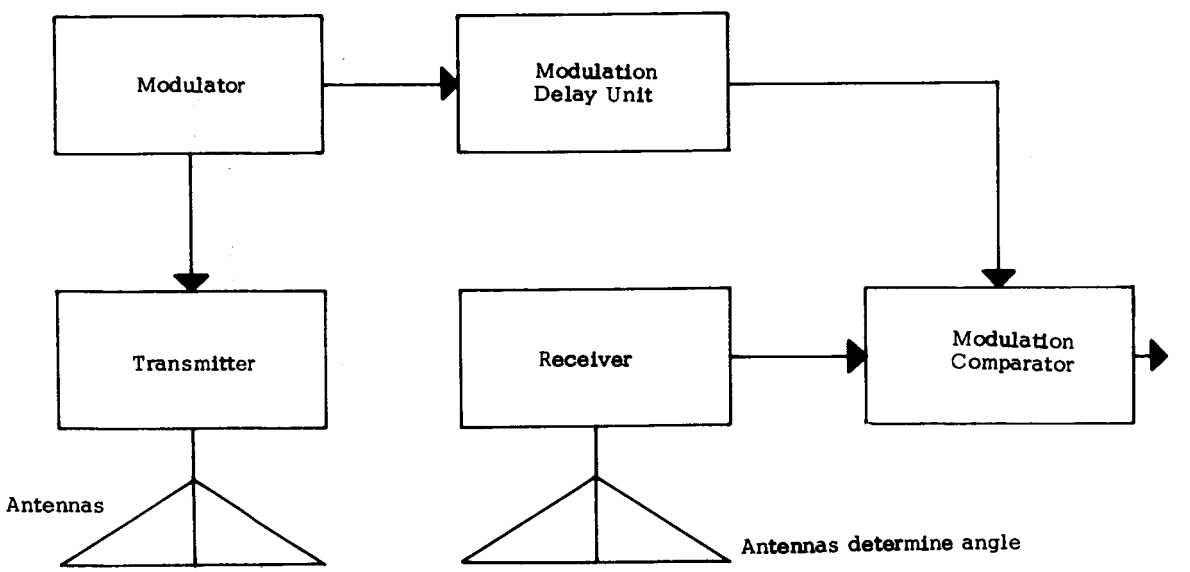

FIGURE 4. Angle-Range-Measurement Scatterometer System

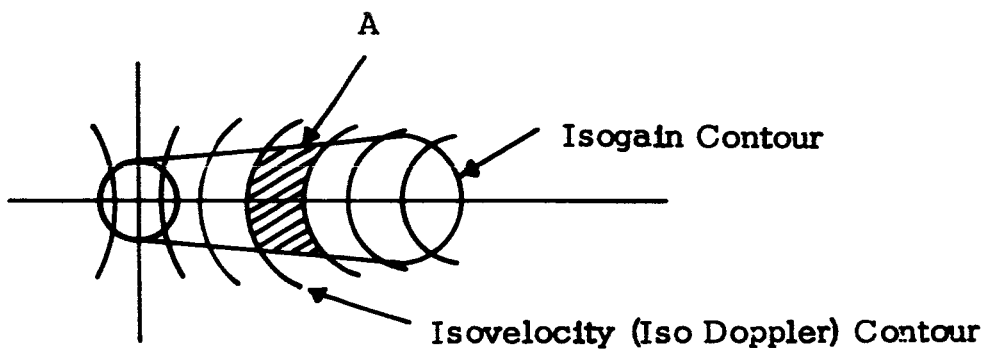

FIGURE 5. Angle-Velocity-Measurement Scatterometer Illuminated Region

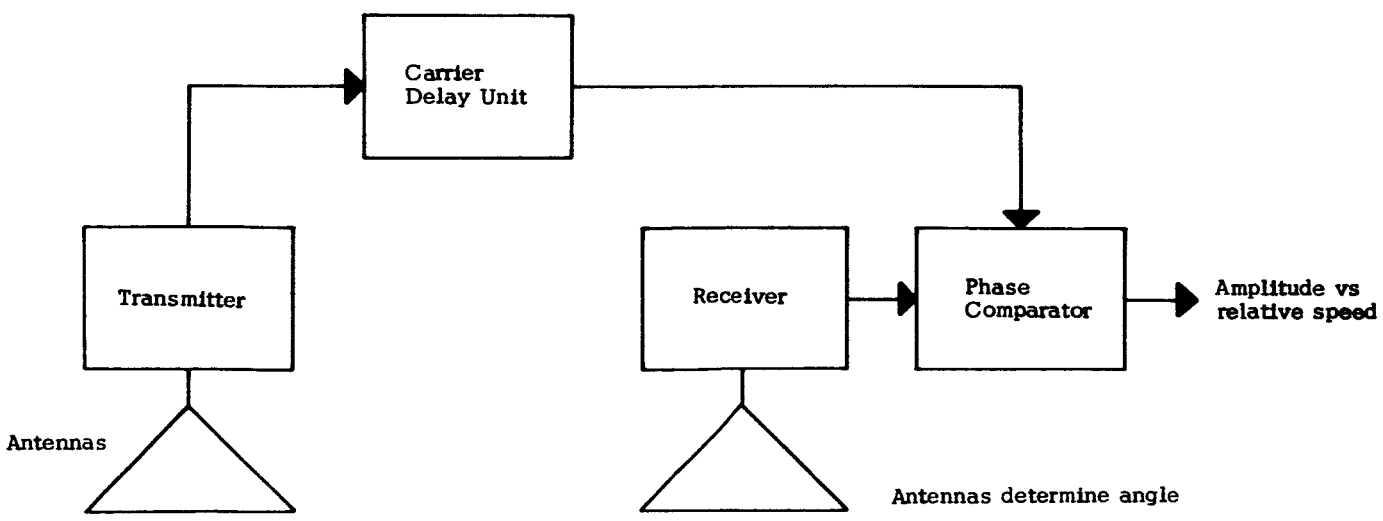

FIGURE 6. Angle-Velocity-Measurement Scatterometer System

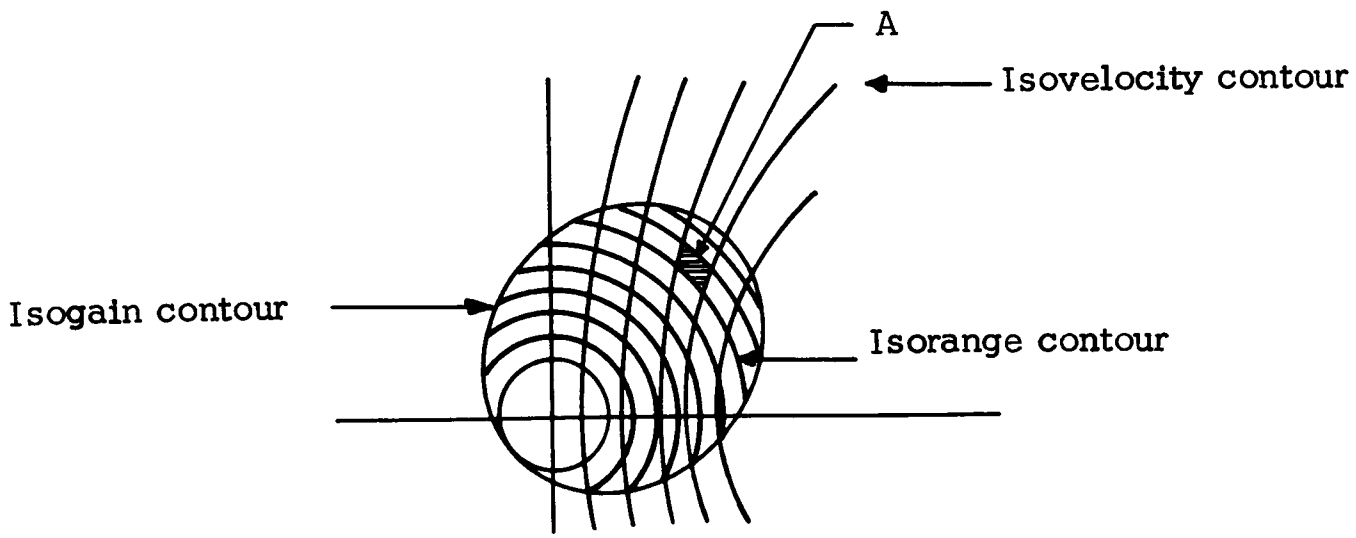

FIGURE 7. Range-Velocity-Measurement Scatterometer Illuminated Region

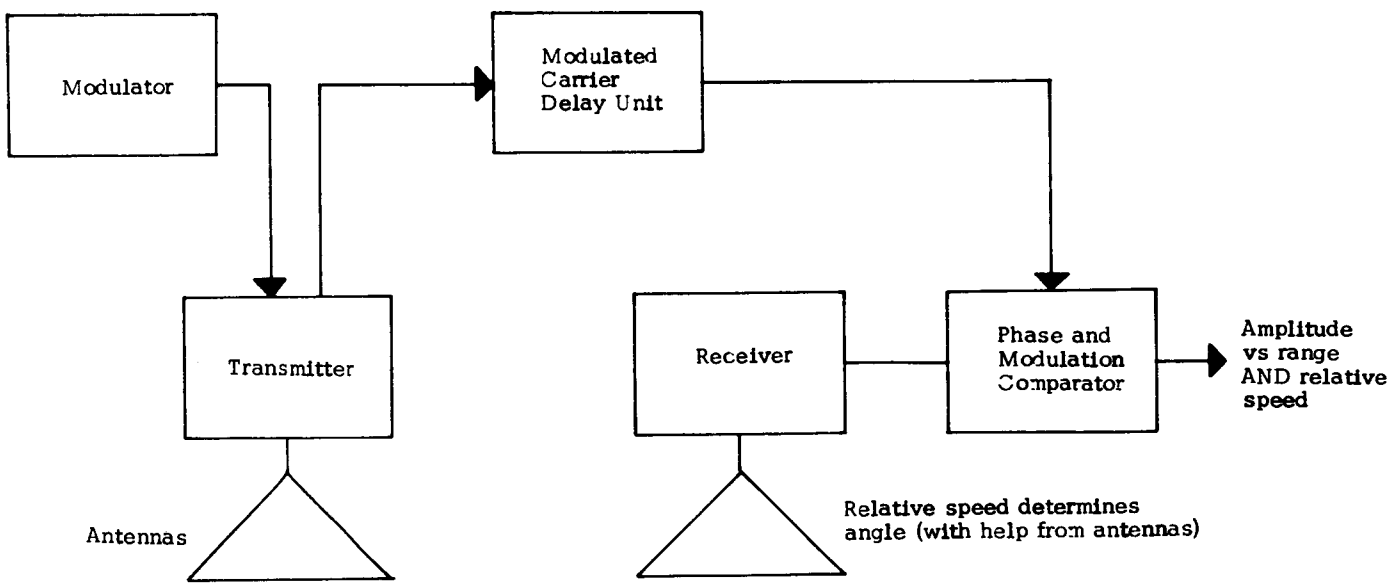

FIGURE 8. Range-Velocity-Measurement Scatterometer System

SCATTEROMETER - ILLUMINATED AREA CHANGE WITH INCREASING TIME FOR FAN-SHAPED ANTENNA BEAM

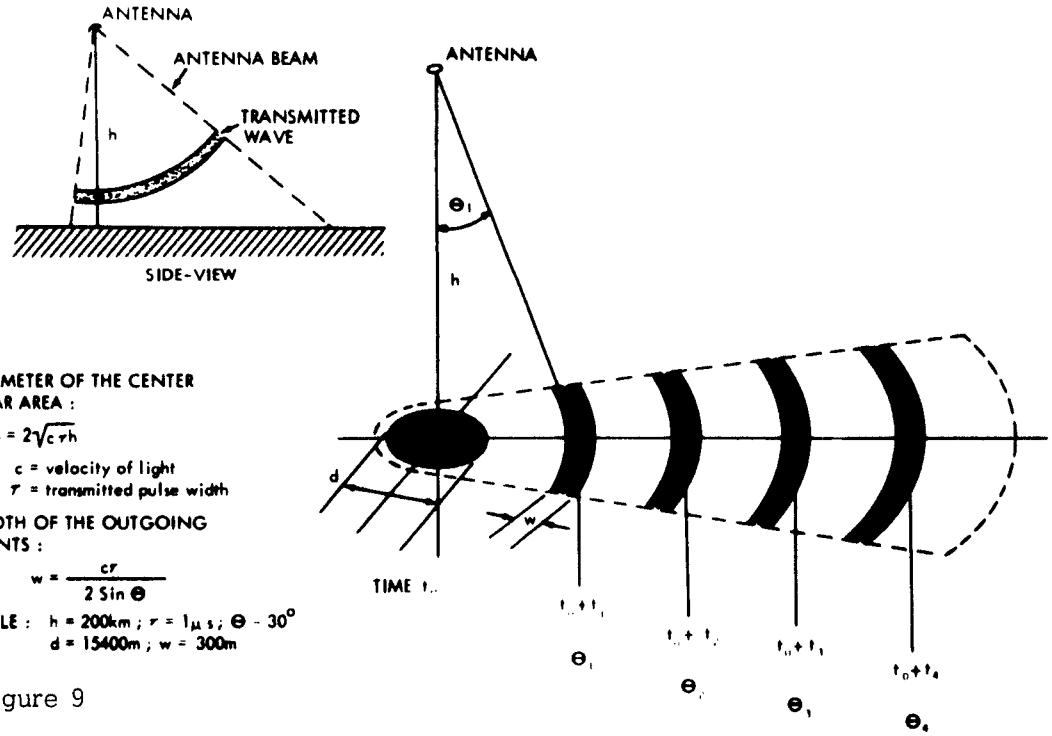

THE DIAMETER OF THE CENTER CIRCULAR AREA :

$$d = 2\sqrt{c\tau h}$$

WHERE : c = velocity of light
τ = transmitted pulse width

THE WIDTH OF THE OUTGOING SEGMENTS :

$$w = \frac{c\tau}{2 \sin \Theta}$$

EXAMPLE : h = 200km ; τ = 1μs ; Θ = 30°
d = 15400m ; w = 300m

Figure 9

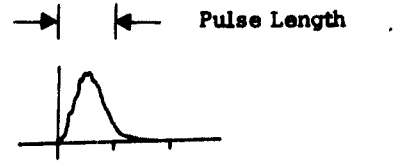

Transmitted Pulse Shape (Not to Scale)

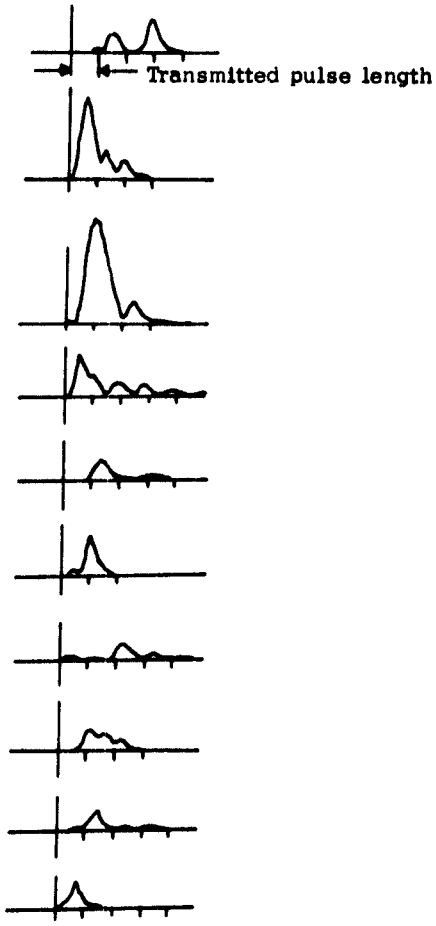

FIGURE 10. Fading for Pulse System

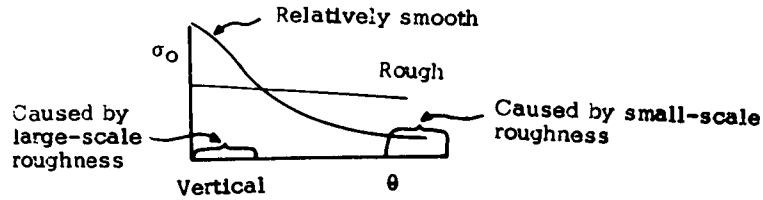

(a) Interpretation

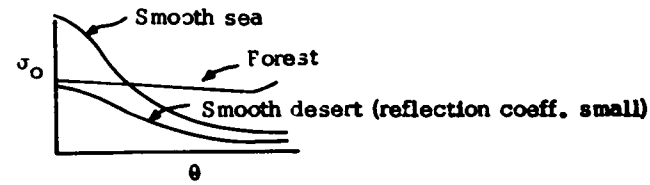

(b) Examples

FIGURE 11. Conclusions of Experiment and Theory

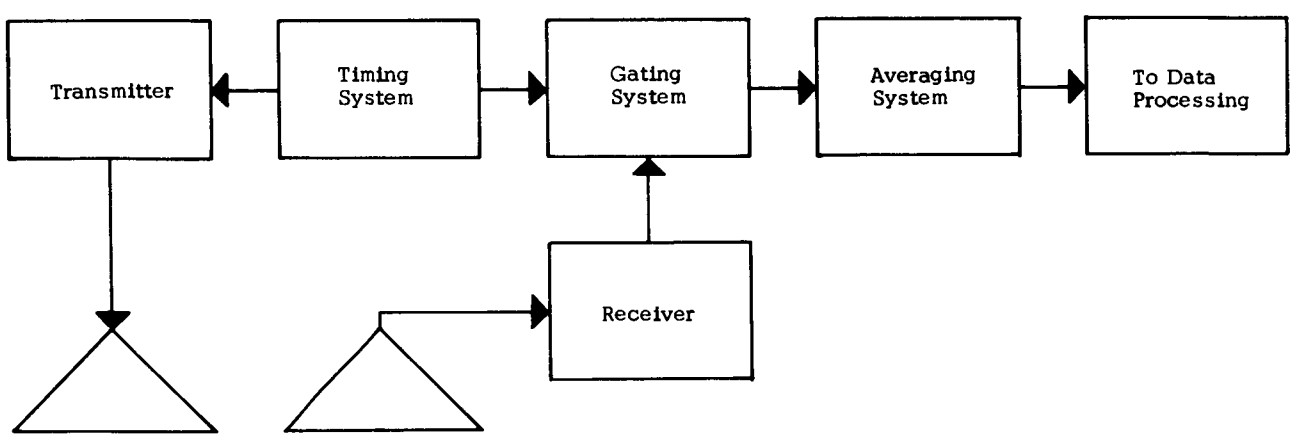

FIGURE 12. Pulse Range-Measurement Scatterometer System

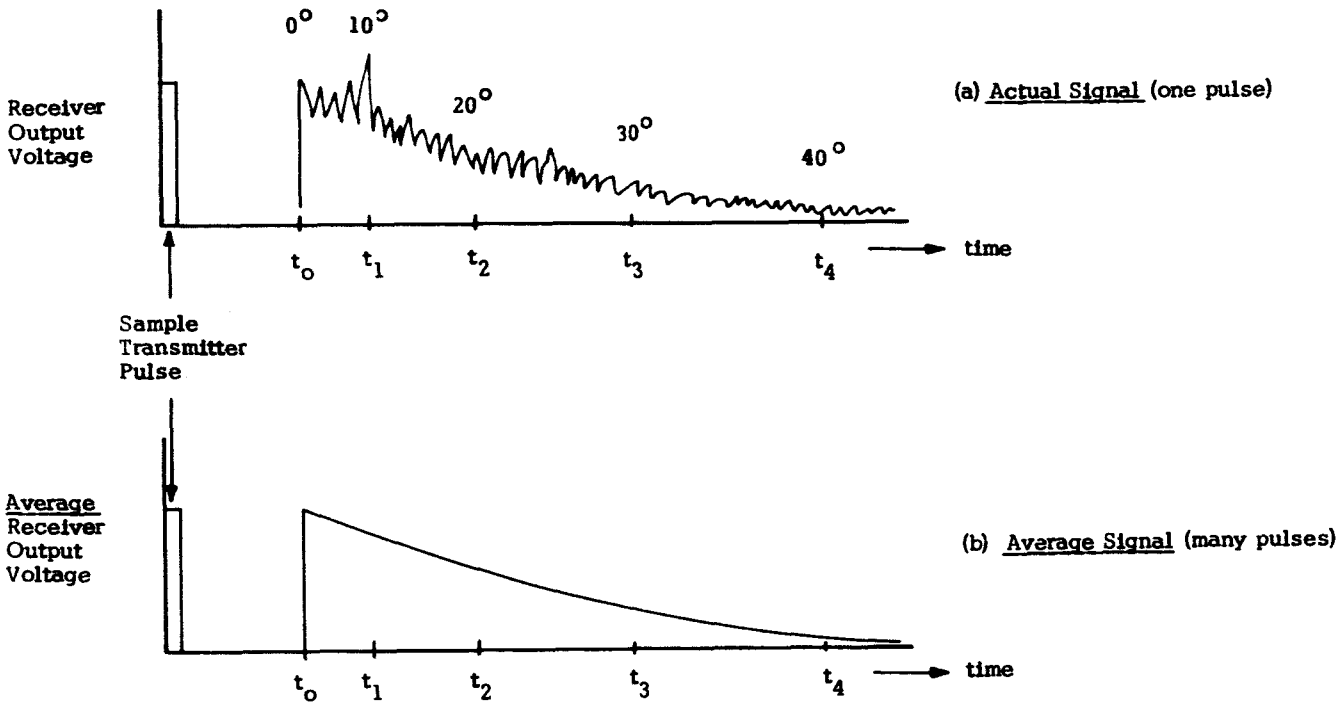

FIGURE 13. Received Pulse -- Fan-Beam Scatterometer

SCATTEROMETER - DATA PROCESSING

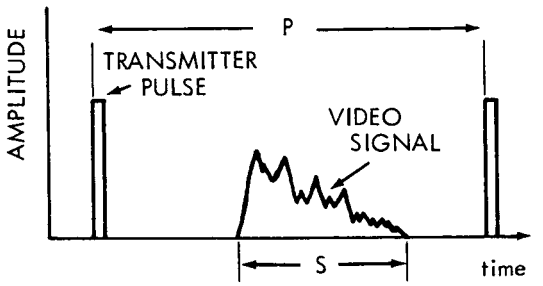

1. RECEIVER OUTPUT

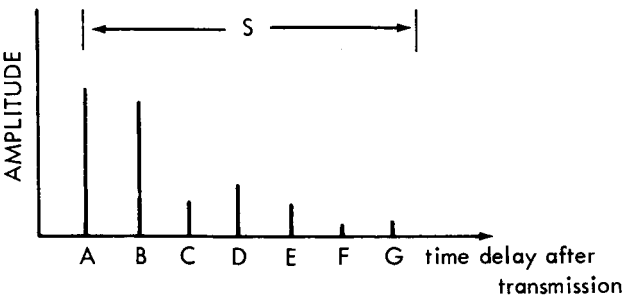

2. VIDEO SIGNAL AMPLITUDE-SAMPLED (ONE TRANSMITTED PULSE)

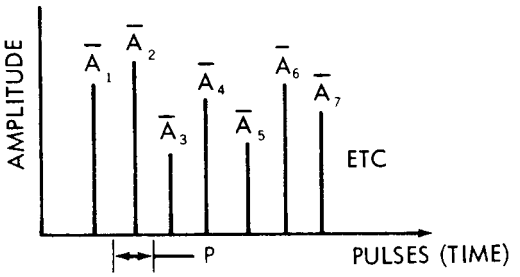

3. AVERAGES OF N TRANSMITTED PULSES EACH SAMPLED AT TIME A.

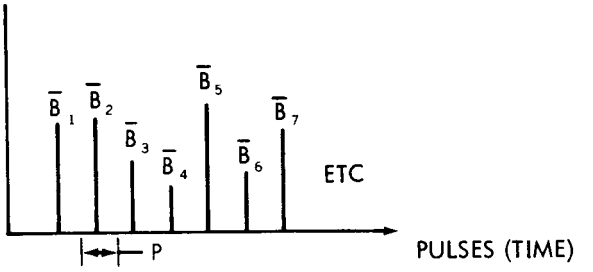

4. AVERAGE OF N TRANSMITTED PULSES EACH SAMPLED AT TIME B.

Figure 14a

SCATTEROMETER - DATA PROCESSING

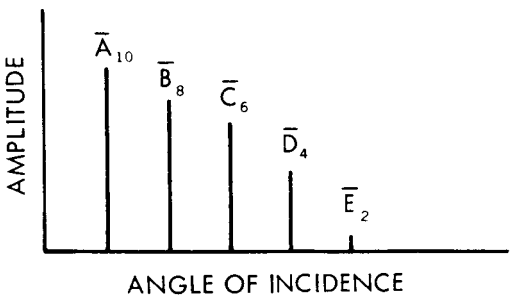

5. COLLECT SAMPLE AVERAGES PERTAINING TO SAME SPOT ON THE TERRAIN. SPOT PASSED FIRST AT TIME G THEN F, E, D, ETC. LAST INFORMATION AT TIME A. TIME A CORRESPONDS TO $\Theta = 0^\circ$

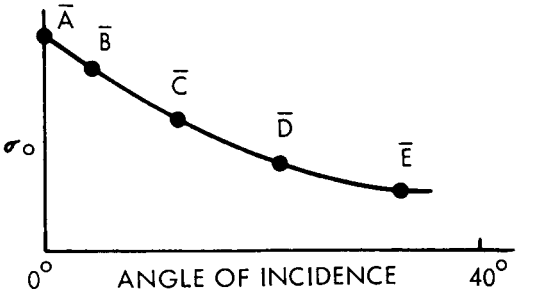

6. SCATTER CURVE = RADAR CROSS SECTION PER UNIT AREA (σ_o) VERSUS ANGLE OF INCIDENCE FOR ONE TERRAIN ELEMENT. σ_o IS PROPORTIONAL TO AMPLITUDE AT TIME A, B, ETC.

Figure 14b

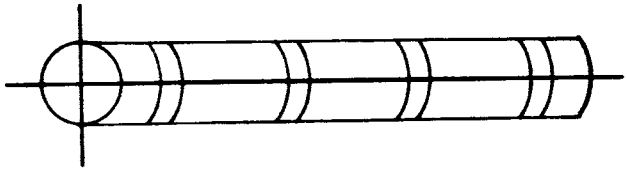

(a) Ideal Ground Illumination

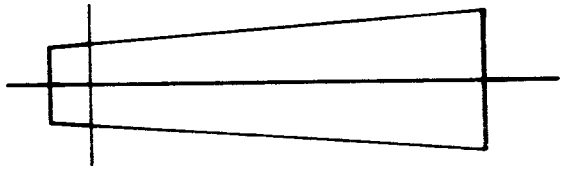

(b) Ground Illumination with Ideal "Square Edge" Pattern

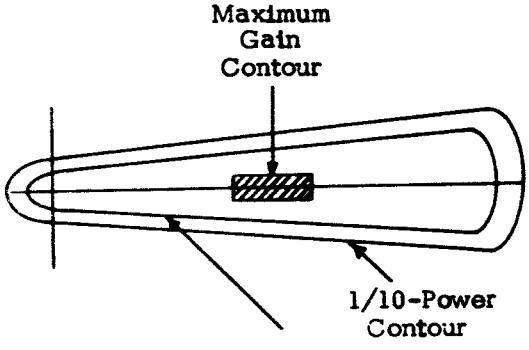

(c) More Realistic Ground Illumination

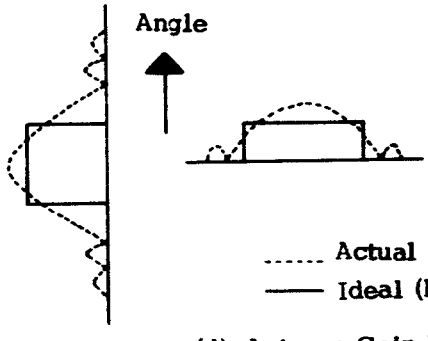

(d) Antenna Gain Pattern Cross-section

FIGURE 15. Ground Illumination

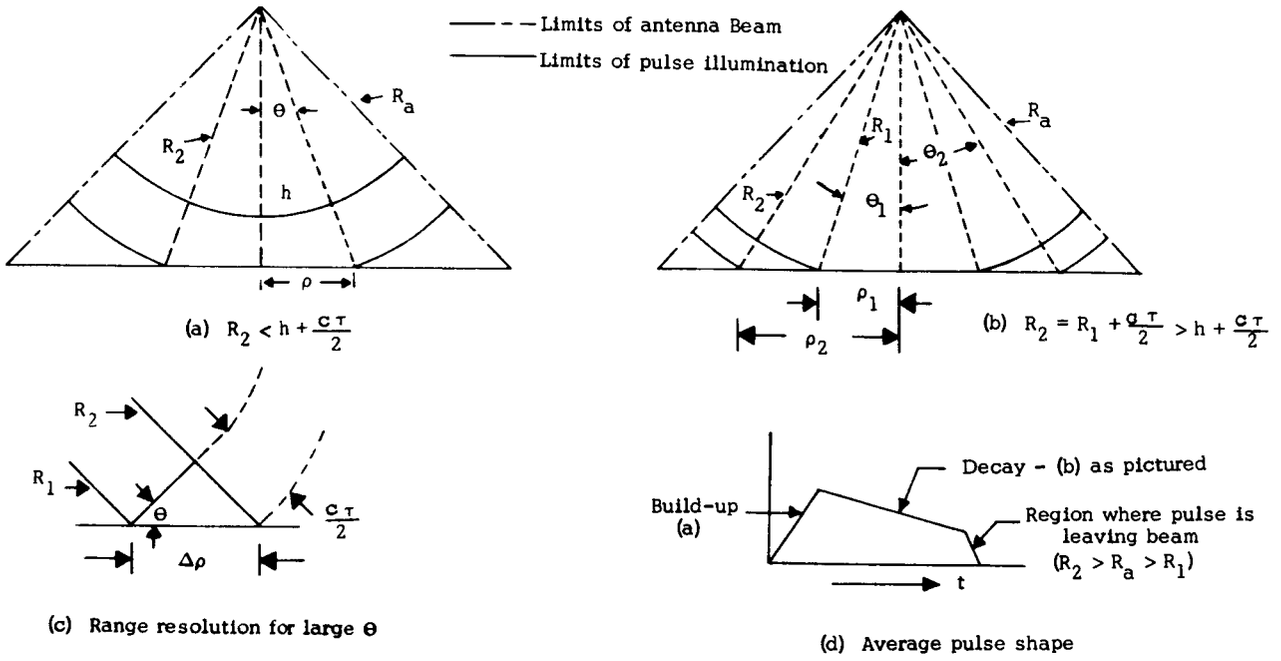

FIGURE 16. Pulse-length Limitation of Illumination

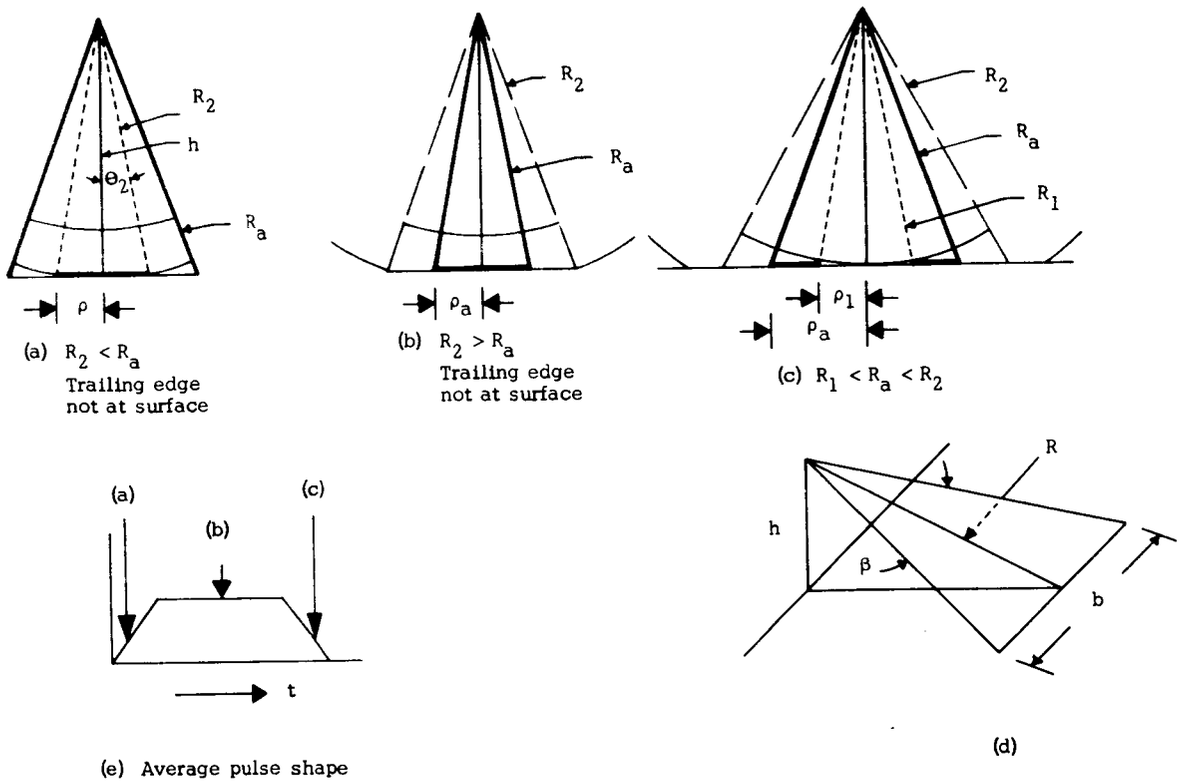

FIGURE 17. Beam-width Limitation of Illumination

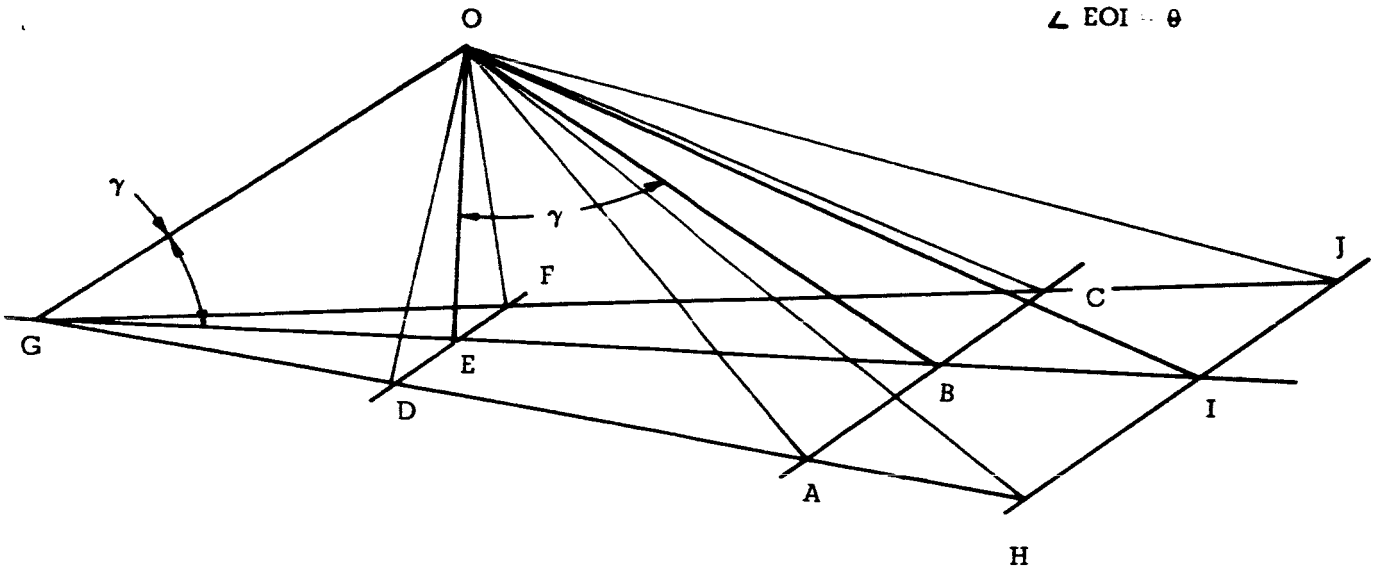

FIGURE 18. Fan-Beam Geometry

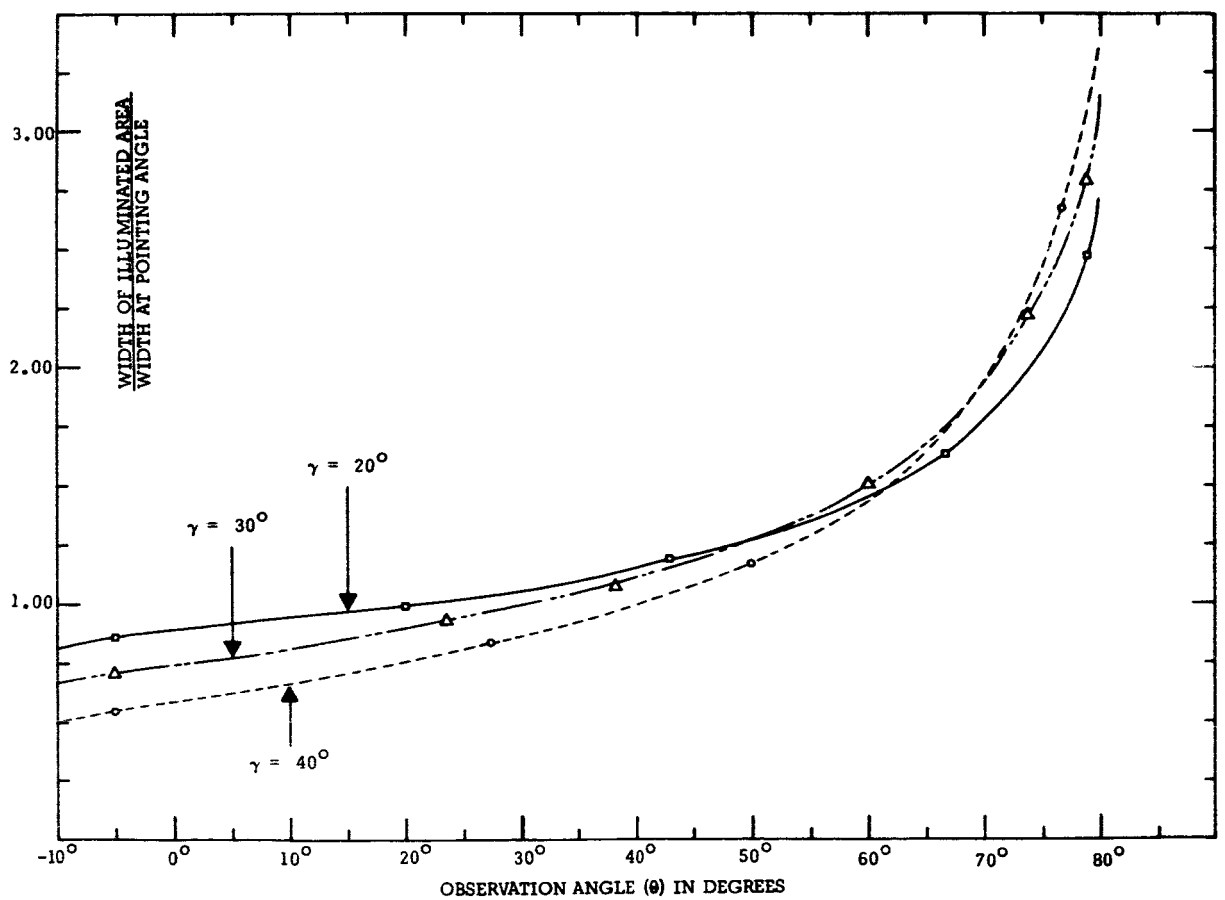

FIGURE 19. Fan-Beam Illuminated Width

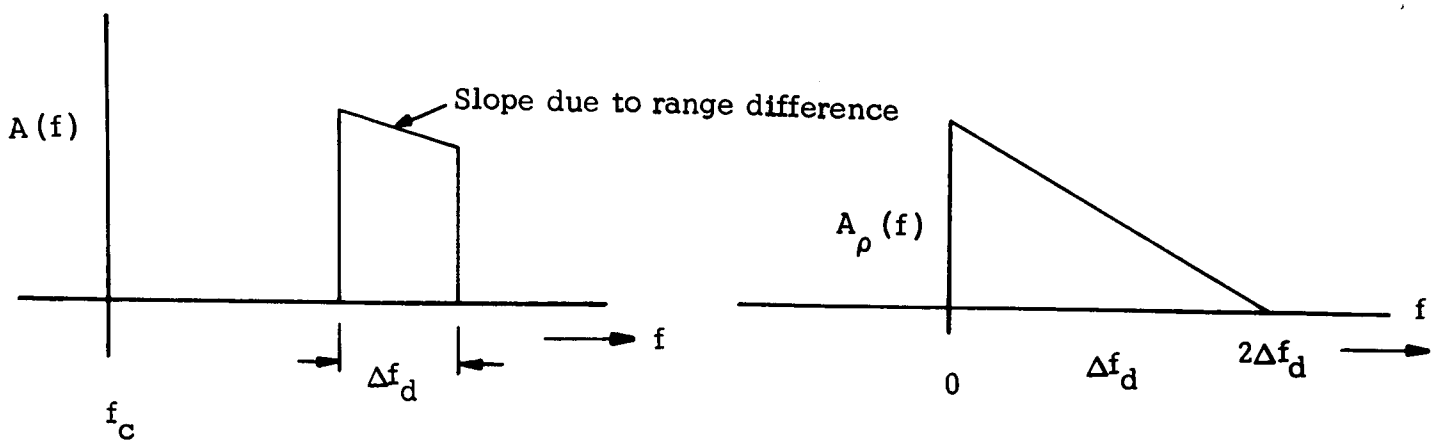

(a) Predetection Spectrum

(b) Post-detection Spectrum

Rectangular Pulse, σ° constant

FIGURE 21. Fading Spectra-Pulse System

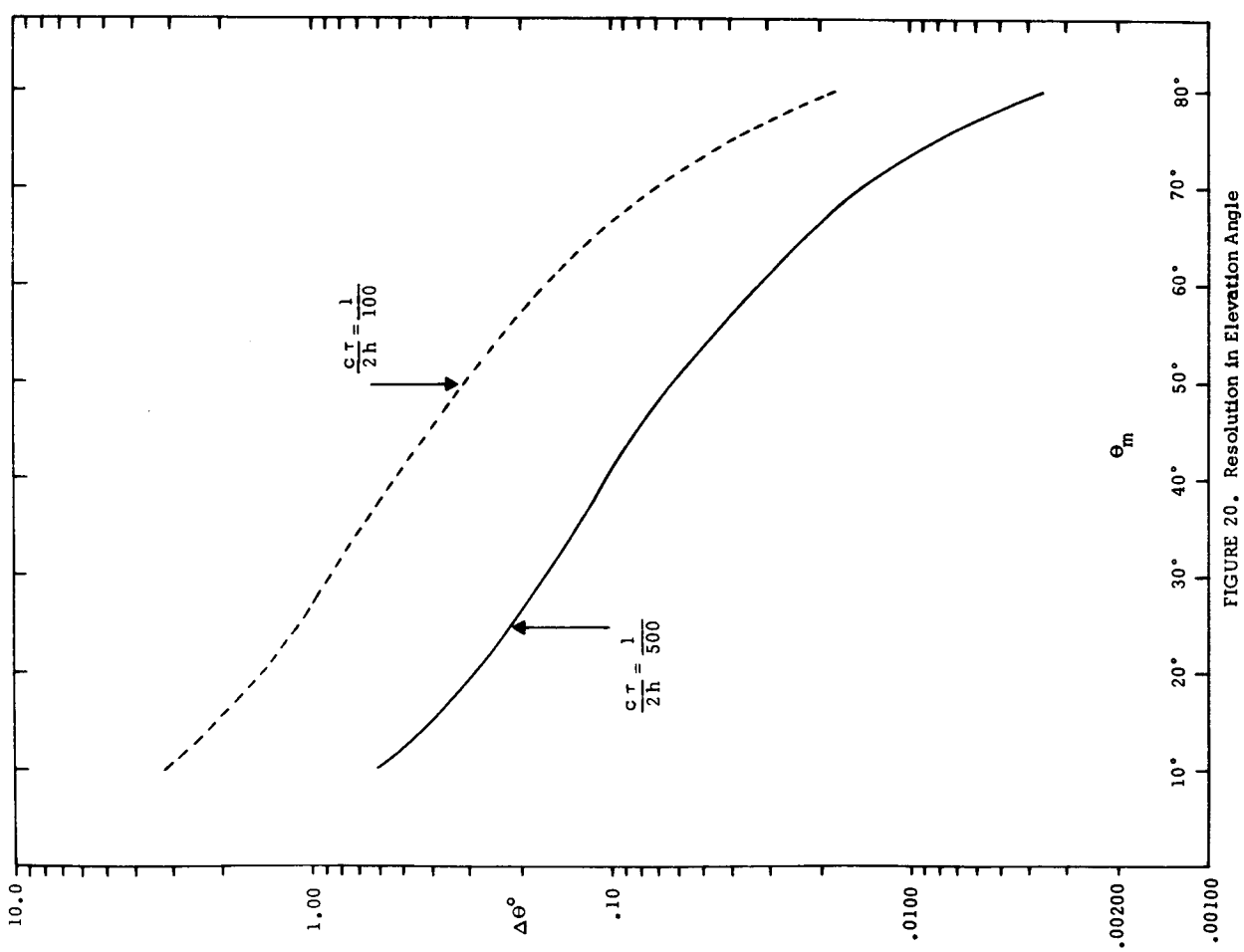

FIGURE 20. Resolution in Elevation Angle

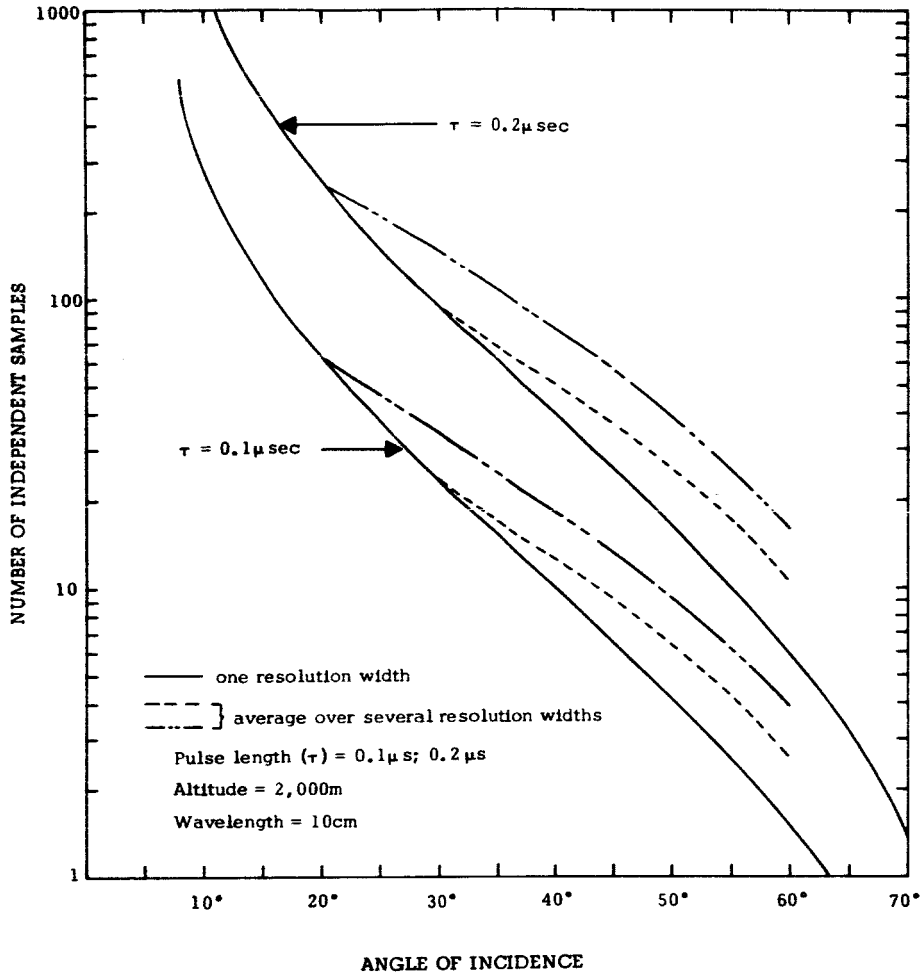

FIGURE 22. Number of Independent Samples - Examples

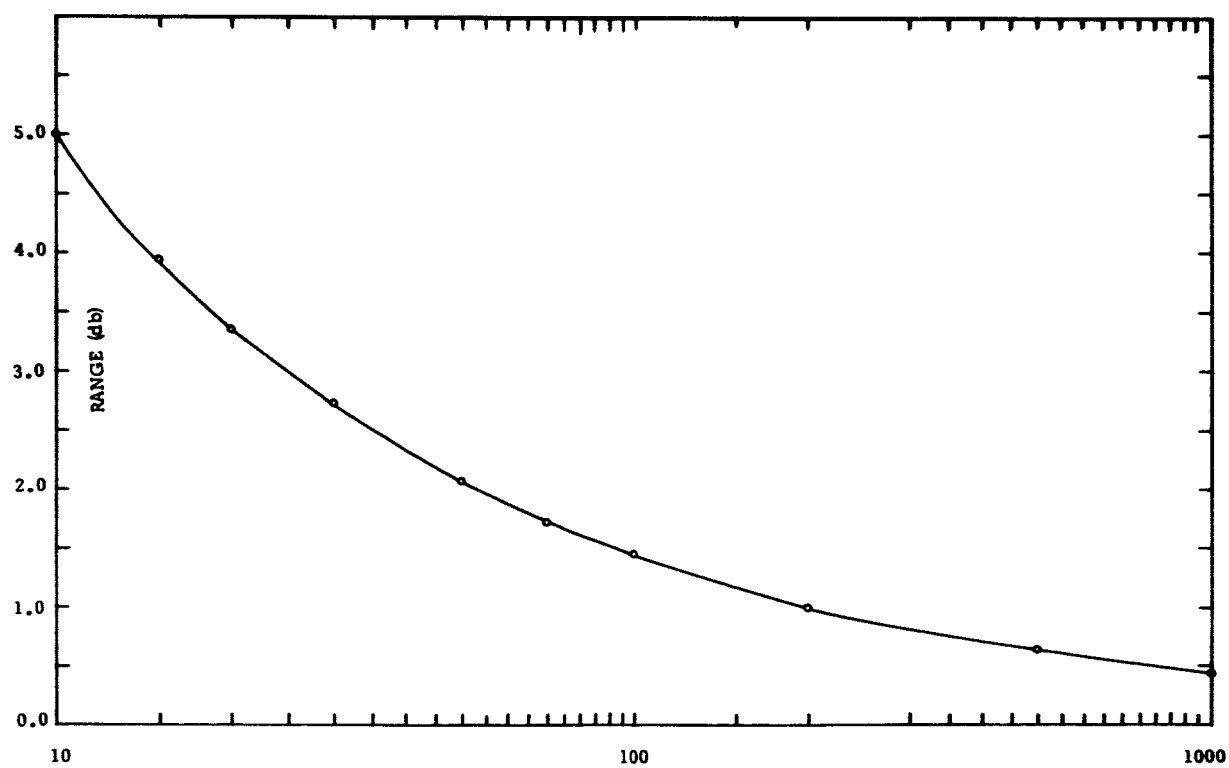

FIGURE 23. Accuracy of Averages

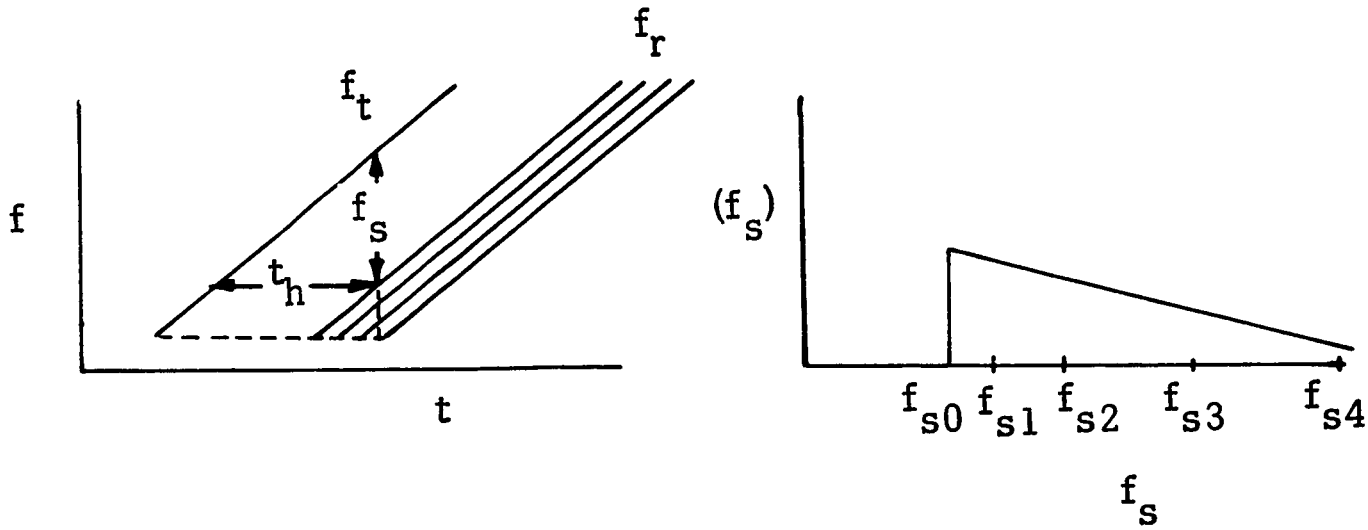

FIGURE 24. Basic FM Principles

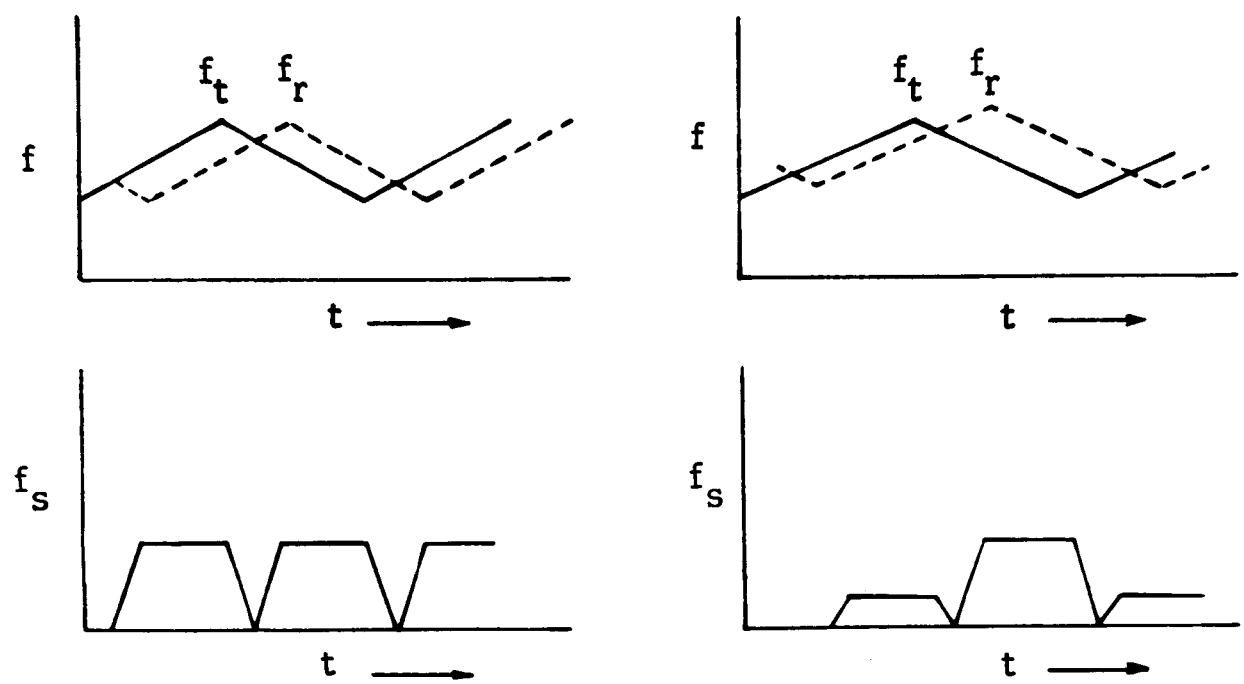

(a) Without Doppler Shift (b) With Doppler Shift

FIGURE 25. Sawtooth Frequency Modulation Waveforms-Single Target

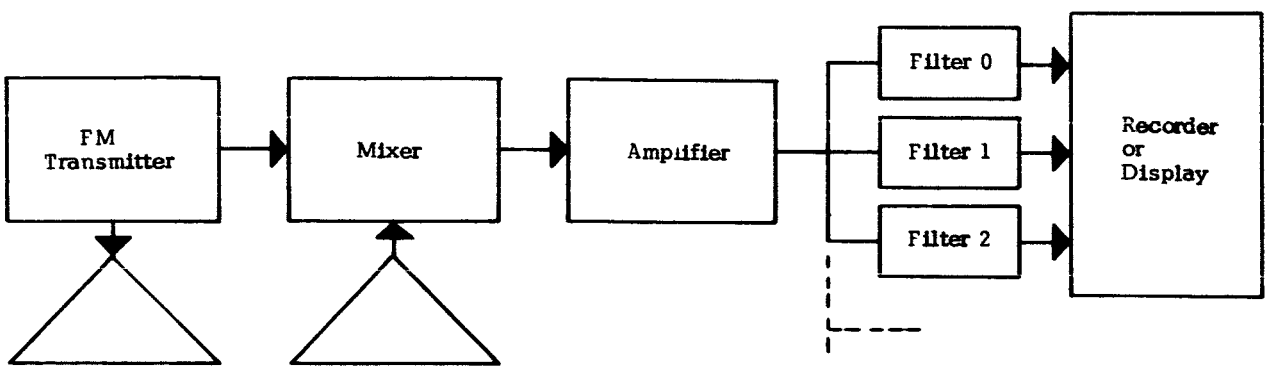

FIGURE 26. Basic FM Scatterometer System

SCATTEROMETER DATA PRESENTATION-POSSIBLE MODES

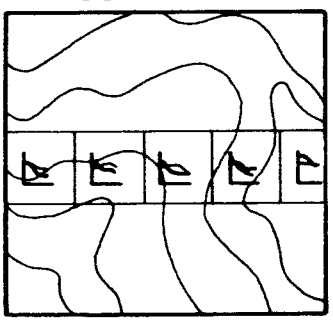

SIGMA VS THETA TWO FREQUENCIES

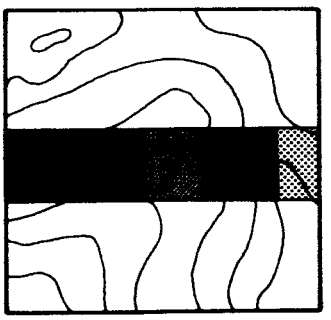

COMBINATION OF PARAMETERS SHOWN AS COLOR (FREQUENCIES, ANGLES, ETC.)

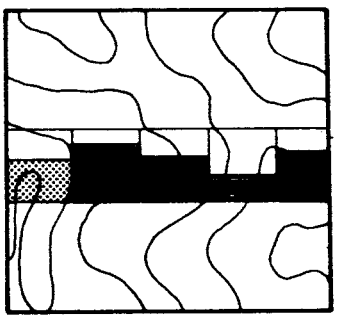

COMBINATIONS SHOWN AS HEIGHT, COLOR, AND INTENSITY

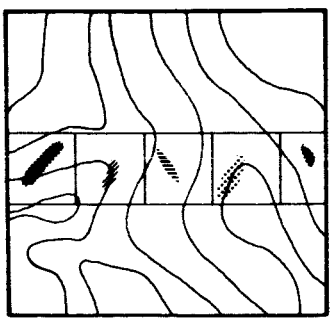

COMBINATIONS SHOWN AS COLOR, LENGTH, WIDTH, AND ANGLE

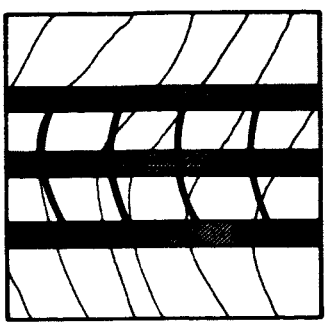

MULTIPLE PASS CONTOURS RELATED BY COLOR

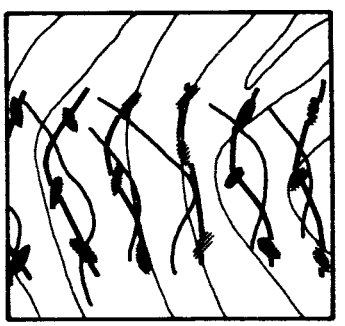

ANGLE PROPERTY CONTOURS RELATED TO COLOR PROPERTY CONTOURS

Figure 27.